Recovery of Dynamical Models of Time-Delay Systems from Time Series: Application to Chaotic Communication

M.D. Prokhorov[1], V.I. Ponomarenko[1,2], A.S. Karavaev[2], B.P. Bezruchko[1,2]

[1] Saratov Branch of the Institute of Radio Engineering and Electronics of Russian Academy of Sciences, Zelyonaya str., 38, Saratov, 410019, Russia
[2] Saratov State University, Astrakhanskaya str., 83, Saratov, 410012, Russia

Abstract

We propose the original methods for reconstructing model delay-differential equations from chaotic time series for various classes of time-delayed feedback systems including: i) scalar time-delay systems with arbitrary nonlinear function, ii) high-order time-delay systems, iii) systems with several coexisting delays, and iv) coupled time-delay systems. These methods are based on the statistical analysis of time intervals between extrema in the time series of time-delay systems and the projection of infinite-dimensional phase space of these systems to suitably chosen low-dimensional subspaces. The methods allow one to recover the delay times, the nonlinear functions, and the parameters characterizing the inertial properties of the systems and to define the a priori unknown order of a time-delay system. In the case of coupled time-delay systems the methods are able to define also the type, strength, and direction of coupling and can be used for the analysis of unidirectional and mutual coupling of time-delay systems for a wide range of the coupling coefficients variation. The proposed methods are efficient for the analysis of short time series under sufficiently high levels of noise. The methods are successfully applied to recovery of standard time-delay systems from their simulated time series corrupted with noise and to modeling various electronic oscillators with delayed feedback from their experimental time series. The proposed methods are applied to the problem of hidden message extraction in the communication systems with nonlinear mixing of information signal and chaotic signal of a time-delay system. Different ways for encryption and decryption of information in these communication schemes are investigated. Using both numerical and experimental data we obtained a high quality of the information signal extraction from the transmitted signal for different message signals and different configurations of the chaotic transmitter with a priori unknown parameters.

1 Introduction

Systems, whose dynamics is affected not only by the current state, but also by past states, are wide spread in nature [1]. Usually these systems are modeled by delay-differential equations. Such models are successfully used in many scientific disciplines, like physics, physiology, biology, economics and cognitive sciences. Typical examples include population dynamics [2], where individuals participate in the reproduction of a species only after maturation, or spatially extended systems, where signals have to cover distances with finite velocities [3]. Within this rather broad class of systems, one can find the Ikeda equation [4] modeling the passive optical resonator system, the Lang-Kobayashi equations [5] describing semiconductor lasers with optical feedback, the Mackey-Glass equation [6] modeling the production of red blood cells, and many other models in biosciences for different phenomena from glucose metabolism to infectious diseases [7].

Generally, the time-delay systems are described by the following equation

$$\varepsilon_n x^{(n)}(t) + \varepsilon_{n-1} x^{(n-1)}(t) + \cdots + \varepsilon_1 \dot{x}(t) = F(x(t), x(t-\tau_1), \ldots, x(t-\tau_k)), \tag{1}$$

where $x(t)$ is the system state at time *t*, $x^{(n)}(t)$ is the time derivative of order *n*, $\tau_1, \ldots, \tau_k$ are the delay times, and $\varepsilon_1, \ldots, \varepsilon_n$ are the parameters characterizing the inertial properties of the system. To uniquely define the system (1) behavior it is necessary to prescribe the initial conditions in the entire time interval $[-\tau_k, 0]$. Therefore, the phase space of the system has to be considered as infinite-dimensional. In fact, even first-order delay-differential equations can possess high-dimensional chaotic dynamics [8]. Thus, the direct reconstruction of the system by the time-delay embedding techniques runs into severe problems. For a successful recovery of the time-delay systems one has to use special methods. The most of them are based on the projection of the infinite-dimensional phase space of time-delay systems onto low-dimensional subspaces [9–18]. These methods use different criteria of quality for the reconstructed equations, for example, the minimal forecast error of the constructed model [9–12], the minimal value of information entropy [13], or various measures of complexity of the projected time series [14–18]. Several methods of time-delay system recovery exploit regression analysis [19–21]. In this chapter we present the original procedure of the delay time reconstruction based on a statistical analysis of time intervals between extrema in the time series and develop further the methods of time-delay system parameter estimation from time series proposed by us recently [22–25] for a more wide class of time-delay systems. The techniques are proposed for reconstructing ring-type time-delay systems from time series of various dynamical variables obtained from different points of the time-delay system.

Until now, the main attention of the researches was focused on the development of methods for reconstruction of single time-delay systems. The problem of recovery of model equations for coupled time-delay systems from time series has not been practically considered yet. At the same time, interaction between time-delay systems is a typical case in many applications. For example, the use of coupled time-delay systems demonstrating chaotic dynamics of a very high dimension is promising for secure communication [26–30], in particular, for chaotic communication systems based on lasers with optical feedback [31–33]. Besides, coupled time-delay differential equations are used for the description of behavior of interacting populations [2, 7, 34] and for modeling the processes in the human cardiovascular system [35, 36]. In this chapter we propose a method that is able to reconstruct two coupled scalar time-delay systems and to estimate the coupling strength and direction from the observed time series data. This method for recovery of coupled time-delayed feedback systems is applied in the chapter to the problem of hidden message extraction in the communication systems with nonlinear mixing of information signal and chaotic signal of a time-delay system.

The chapter is organized as follows. In Sec. II we consider peculiarities of extrema location in the time series of time-delay systems. In Sec. III the method for reconstruction of first-order time-delay systems is presented. The method is applied to recovery of time-delay differential equations from their simulated time series corrupted with noise and to modeling experimental system with delay-induced dynamics from chaotic time series. Different criteria of quality for the recovered equations are considered. In Sec. IV we propose the method for reconstructing ring-type time-delay systems from time series of various dynamical variables obtained from different points of the time-delay system. The method for reconstructing high-order time-delay systems is presented in Sec. V. The method efficiency is illustrated using various simulated and experimental time series. Sec. VI describes the technique for determining the a priori unknown order of a time-delay system. The recovery of time-delay systems with two coexisting delays is considered in Sec. VII. In Sec. VIII the method for reconstruction of coupled time-delay systems is proposed. We verify our method using both numerical and experimental data. In Sec. IX we apply the proposed methods to extracting the hidden message in the communication systems with nonlinear mixing of information signal and chaotic signal of a time-delay system. The message extraction procedure is illustrated using both numerical and experimental data for different configurations of the transmitter and different kinds of information signals. In Sec. X we summarize our results.

2 Peculiarities of Time-Delay System Time Series

Statistical analysis of time intervals between extrema in time series of various model and real time-delay systems reveals the following general regularities. If the system has inertial properties, the dependence of number N of pairs of extrema in its time series separated in time by τ on the value of τ demonstrates a pronounced minimum at the level of the delay time of the system [Fig. 1(a)]. Let us explain the qualitative features of $N(\tau)$ with one of the most popular delay-differential equation

$$\varepsilon_1 \dot{x}(t) = -x(t) + f(x(t-\tau_1)) . \tag{2}$$

In general case Eq. (2) is a mathematical model of an oscillating system composed of a ring with three ideal elements: nonlinear, delay, and inertial ones (Fig. 2). In the presence of inertial properties ($\varepsilon_1 > 0$), which corresponds to real situations, the extrema in $x(t)$ are close to quadratic ones and therefore $\dot{x}(t) = 0$ and $\ddot{x}(t) \neq 0$ at the extremal points. In fact, the condition $\dot{x}(t) = \ddot{x}(t) = 0$ is satisfied for a point, which is a point of inflection, or a non-quadratic extremum, or belongs to an interval of constant value of the dynamical variable. But the presence of inertial properties in the system prevents the implementation of these conditions. It can be shown that in this case there are practically no extrema in $x(t)$ separated in time by the delay time τ_1. Differentiation of Eq. (2) with respect to t gives

$$\varepsilon_1 \ddot{x}(t) = -\dot{x}(t) + \frac{df(x(t-\tau_1))}{dx(t-\tau_1)} \dot{x}(t-\tau_1) . \tag{3}$$

If for $\dot{x}(t) = 0$ in a typical case $\ddot{x}(t) \neq 0$, then, as it can be seen from Eq. (3), for $\varepsilon_1 \neq 0$ the condition $\dot{x}(t-\tau_1) \neq 0$ must be fulfilled. Thus, there must be no extremum separated in time by τ_1 from a quadratic extremum and, hence, $N(\tau_1) \to 0$. For $\tau \neq \tau_1$, the derivatives $\dot{x}(t)$ and $\dot{x}(t-\tau)$ can be simultaneously equal to zero, i.e., it is possible to find extrema separated in time by τ. Note that for chaotic temporal realizations of the systems under investigation practically all critical points with $\dot{x}(t)=0$ are the extremal ones, and therefore we call the points with $\dot{x}(t)=0$ the extremal points throughout this chapter.

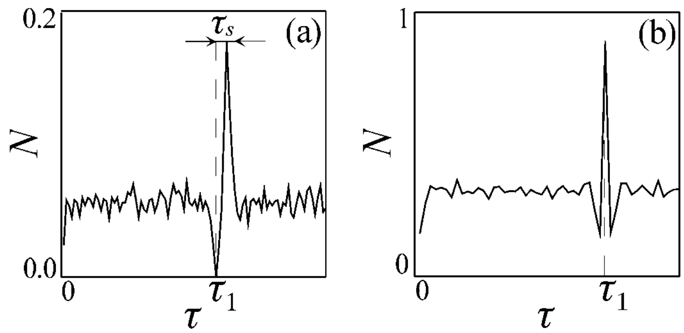

Figure 1. Typical dependence of number N of pairs of extrema in chaotic time series of a time-delay system separated in time by τ on the value of τ in the presence of inertial properties in the system (a) and in the absence of inertial properties (b). $N(\tau)$ is normalized to the total number of extrema in time series.

Similar properties are inherent in a more general class of time-delay systems

$$\dot{x}(t)=F(x(t),x(t-\tau_1)). \tag{4}$$

Time differentiation of Eq. (4) gives

$$\ddot{x}(t)=\frac{\partial F(x(t),x(t-\tau_1))}{\partial x(t)}\dot{x}(t)+\frac{\partial F(x(t),x(t-\tau_1))}{\partial x(t-\tau_1)}\dot{x}(t-\tau_1). \tag{5}$$

Similarly to Eq. (3), Eq. (5) implies that in a typical case of quadratic extrema derivatives $\dot{x}(t)$ and $\dot{x}(t-\tau_1)$ do not vanish simultaneously, i.e., if $\dot{x}(t)=0$, then $\dot{x}(t-\tau_1)\neq 0$.

In the absence of inertial properties ($\varepsilon_1=0$) differentiation of Eq. (2) with respect to *t* gives

$$\dot{x}(t)=\frac{df(x(t-\tau_1))}{dx(t-\tau_1)}\dot{x}(t-\tau_1) \tag{6}$$

From Eq. (6) it follows that if $\dot{x}(t-\tau_1)=0$, then $\dot{x}(t)=0$. Thus, for $\varepsilon_1=0$ every extremum of $x(t)$ is followed within the time τ_1 by the extremum. As the result, $N(\tau)$ shows a maximum for $\tau=\tau_1$ [Fig. 1(b)].

The situation in the absence of inertial properties can be pictorially shown with the help of a ring circuit (Fig. 2), for which the condition $\varepsilon_1=0$ is equivalent to the lack of filter and the unbounded passband of other elements. The signal $x(t)$ propagates through the ring in one direction and in the process the delay element provides the signal delay for τ_1 and the nonlinear element transforms the signal in accordance with its transfer function $f(x(t-\tau_1))$. In this case the signal at the nonlinear element output is defined at the time *t* only by the signal at the delay element input at the time $t-\tau_1$. Hence, the time evolution of the points of $x(t)$ can be represented by the iteration diagram of the one-dimensional map $x(t-\tau_1)\to x(t)$ in Fig. 3(a), where one step of discrete time corresponds to the time shift τ_1 in the continuous time. Graphical plotting of the mapping of several neighbor points chosen in $x(t)$ in the neighborhood of extremum [Fig. 3(b)] indicates that an extremum always maps into the extremum. From Fig. 3 it follows that the number of extrema separated in time by τ slightly differing from τ_1 must be relatively small resulting in the presence of minima in Fig. 1(b). In actuality we have to deal not with the continuous $x(t)$ realization but with a discrete time series $\{x_t\}_{t=1}^{M}$ obtained as a result of numerical solution of differential equation or experimental measurement of the system state x at the discrete time points. However, as can be seen from Fig. 3(b), in this case the situation is also typical, when an extreme point of the time series is followed by the extremum within the time τ_1.

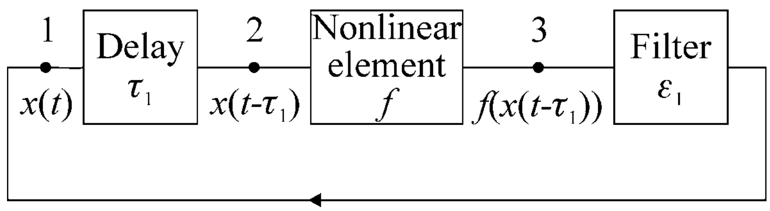

Figure 2. Block scheme of a ring system with nonlinear time-delayed feedback. Numerals designate points where a dynamical variable can be measured.

If the system has a bounded bandpass ($\varepsilon_1 > 0$), which corresponds to real situations, the most probable value of the time interval between extrema in $x(t)$ shifts from τ_1 a to larger values and the extrema can be found most often at the distance $\tau_1 + \tau_s$ apart [Fig. 1(a)]. For instance, the computational investigation of Eq. (2) with quadratic nonlinear function $f(x) = \lambda - x^2$ allows us to obtain an estimation $\tau_s \approx \varepsilon_1 / 2$ for large values of the parameter of nonlinearity λ.

The presence of noise in time series brings into existence spurious extrema that are not caused by the intrinsic dynamics of a time-delay system. Thus, owing to high-frequency noise a probability to find a pair of extrema in time series separated in time by τ has to increase in general. As a result, with noise increasing the average N value becomes greater. The probability to find a pair of extrema separated by the interval τ_1 also increases. However, for moderate noise levels this probability is still less than the probability to find a pair of extrema separated in time by $\tau \neq \tau_1$. Hence, the qualitative features of the $N(\tau)$ plot specified by the delay-induced dynamics are retained for a moderate noise level.

3 Reconstruction of First-Order Time-Delay Systems

Let us consider the procedure of first-order time-delay system recovery with Eq. (2) as an example. To define the delay time τ_1 one has to determine the extrema in the time series and after that to define for different values of time τ the number N of pairs of extrema separated in time by τ and to construct the $N(\tau)$ plot. The absolute minimum of $N(\tau)$ located near the absolute maximum is observed at the delay time τ_1. Note that this method of the delay time definition uses only operations of comparing and adding. It needs neither ordering of data, nor calculation of approximation error or certain measure of complexity of the trajectory and therefore it does not need significant time of computation. The dependence of accuracy of the delay time recovery on the step of τ variation and the time series length is considered in Ref. [22].

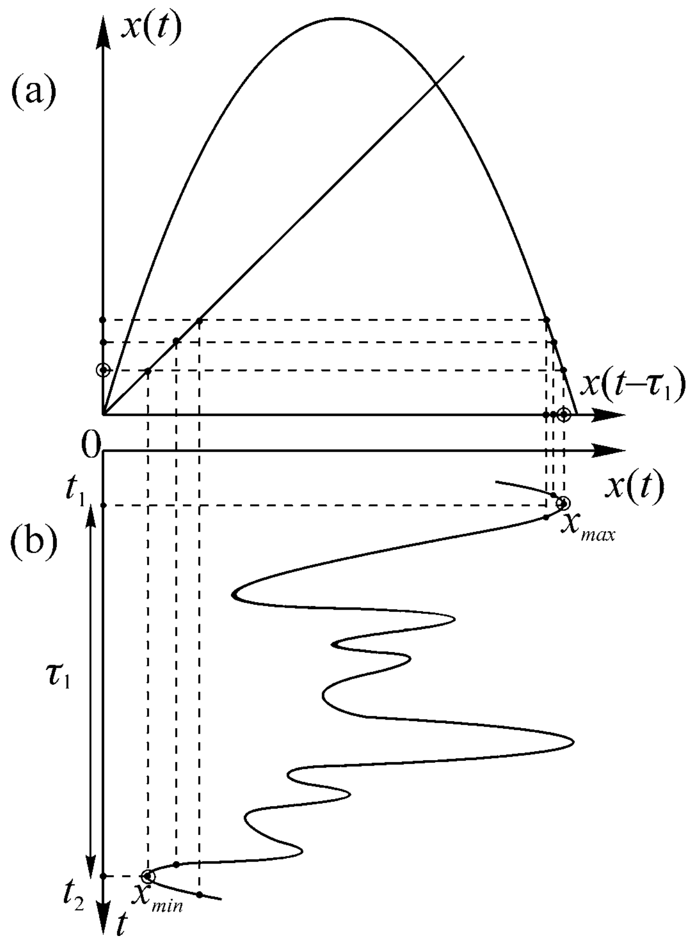

Figure 3. (a) Quadratic transfer function of the nonlinear element and mapping of input signal points into output. (b) Signal temporal realization with the time series points (dots) shown in the neighborhood of two extremal points (circles).

To recover the parameter ε_1 and the nonlinear function *f* from the chaotic time series let us rewrite Eq. (2) as

$$\varepsilon_1 \dot{x}(t) + x(t) = f(x(t - \tau_1)) . \tag{7}$$

Thus, it is possible to reconstruct the nonlinear function by plotting in a plane a set of points with coordinates $(x(t-\tau_1), \varepsilon_1 \dot{x}(t) + x(t))$. Since the parameter ε_1 is a priori unknown, one needs to plot $\varepsilon_1 \dot{x}(t) + x(t)$ versus $x(t-\tau_1)$ under variation of ε, searching for a single-valued dependence in the $(x(t-\tau_1), \varepsilon \dot{x}(t) + x(t))$ plane, which is possible only for $\varepsilon = \varepsilon_1$. As a quantitative criterion of single-valuedness in searching for ε_1 we use the minimal length of a line $L(\varepsilon)$ connecting all points ordered with respect to $x(t-\tau_1)$ in the plane $\left(x(t-\tau_1), \varepsilon\dot{x}(t)+x(t)\right)$. The minimum of $L(\varepsilon)$ is observed at $\varepsilon=\varepsilon_1$. The set of points constructed for the defined ε_1 in the plane $\left(x(t-\tau_1), \varepsilon_1\dot{x}(t)+x(t)\right)$ reproduces the nonlinear function, which can be approximated if necessary. In contrast to methods presented in Refs. [15,16], which use only extremal points or points selected according to a certain rule for the nonlinear function recovery, the proposed technique uses all points of the time series. It allows one to estimate the parameter ε_1 and to reconstruct the nonlinear function from short time series even in the regimes of weakly developed chaos.

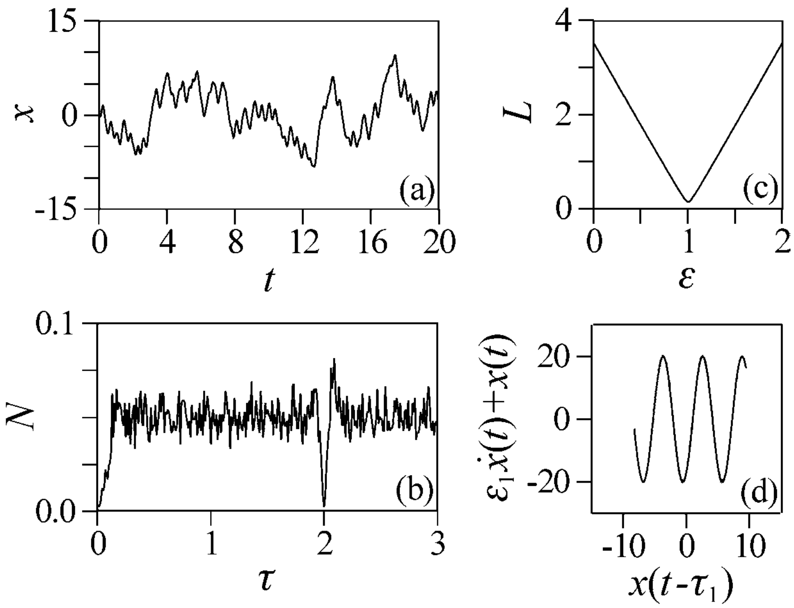

Figure 4. (a) The time series of the Ikeda equation (8). (b) Number N of pairs of extrema in the time series separated in time by τ, as a function of τ. $N(\tau)$ is normalized to the total number of extrema in the time series. $N_{\min}(\tau)=N(2.00)$ (c) Length L of a line connecting all points ordered with respect to $x(t-\tau_1)$ in the $\left(x(t-\tau_1), \varepsilon\dot{x}(t)+x(t)\right)$ plane, as a function of ε. $L(\varepsilon)$ is normalized to the number of points in the plane. $L_{\min}(\varepsilon)=L(1.00)$. (d) The recovered nonlinear function.

To test the efficiency of the proposed technique we have used it to reconstruct the equations of various time-delay systems having the form of Eq. (2) from the time series gained from their numerical solution. In particular, we apply the method to a time series of the Ikeda equation [4]

$$\dot{x}(t)=-x(t)+\mu\sin(x(t-\tau_1)-x_0) \tag{8}$$

modeling the passive optical resonator system. The Ikeda equation (8) has the form of Eq. (2) with $\varepsilon_1=1$. The parameters of the system (8) are chosen to be $\mu=20$, $\tau_1=2$, and $x_0=\pi/3$ to produce a dynamics on a high-dimensional chaotic attractor [3]. Part of the time series is shown in Fig. 4(a). The time series is sampled in such a way that 200 points in time series cover a period of time equal to the delay time $\tau_1=2$. The data set consists of 20000 points and exhibits about 1100 extrema.

For various τ values we count the number *N* of situations when $\dot{x}(t)$ and $\dot{x}(t-\tau)$ are simultaneously equal to zero and construct the $N(\tau)$ plot [Fig. 4(b)]. The step of τ variation in Fig. 4(b) is equal to the integration step $h = 0.01$. The time derivatives $\dot{x}(t)$ are estimated from the time series by applying a local parabolic approximation. The absolute minimum of $N(\tau)$ takes place exactly at $\tau = \tau_1 = 2.00$. To construct the $L(\varepsilon)$ plot [Fig. 4(c)] the step of ε variation is also set by 0.01. The minimum of $L(\varepsilon)$ takes place accurately at $\varepsilon = \varepsilon_1 = 1.00$. In Fig. 4(d) the recovered nonlinear function is shown. It coincides practically with the true function of Eq. (8). Note that for the construction of the $L(\varepsilon)$ plot and for the recovery of the multimodal function *f* we use only 2000 points of the time series. For the approximation of the recovered function we use polynomials of different degree. The sinusoid amplitude [Fig. 4(d)] allows one to define the parameter μ of Eq. (8). The parameter x_0 can be calculated from the function value at $x(t-\tau_1) = 0$. The approximation of the recovered function with a polynomial of degree 20 allows us to obtain the following estimation: $\mu' = 19.94$ and $x_0' = 1.046$ $(\pi/3 \approx 1.047)$.

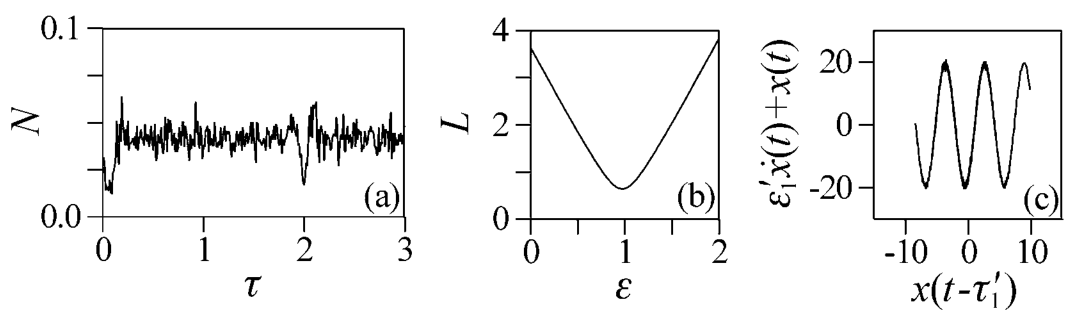

Figure 5. Reconstruction of the Ikeda equation in the presence of a 20% additive noise. (a) The $N(\tau)$ plot. $N_{\min}(\tau) = N(2.00)$. (b) The $L(\varepsilon)$ plot. $L_{\min}(\varepsilon) = L(0.98)$. (c) The recovered nonlinear function.

To investigate the robustness of the method to perturbations we apply it to the data produced by adding a zero-mean Gaussian white noise to the time series of Eq. (8). For the case where the additive noise has a standard deviation of 20% of the standard deviation of the data without noise (the signal-to-noise ratio is about 14 dB) the location of the minimum of $N(\tau)$ still allows us to estimate the delay time accurately, $\tau_1' = 2.00$ [Fig. 5(a)]. The minimum of $L(\varepsilon)$ takes place at $\varepsilon_1' = 0.98$ [Fig. 5(b)]. The nonlinear function recovered using the estimated values τ_1' and ε_1' is shown in Fig. 5(c). In spite of sufficiently high noise level and inaccuracy of estimation of ε_1 the recovery of the nonlinear function has a good quality, which is significantly higher than that reported in Ref. [21] for the same parameter values of the Ikeda equation with noise.

The second example is the method application to experimental time series of the electronic oscillator with delayed feedback. In the block representation of this oscillator (Fig. 2) a delay for time τ_1 is provided by a delay line, the role of nonlinear element is played by an amplifier with the transfer function f and the system inertial properties are defined by a filter, which parameters specify ε_1. For the case when the filter is a low-frequency first-order RC-filter such oscillator is given by

$$RC\dot{V}(t) = -V(t) + f(V(t-\tau_1)), \qquad (9)$$

where $V(t)$ and $V(t-\tau_1)$ are the delay line input and output voltages, respectively; R and C are the resistance and capacitance of the filter elements. Equation (9) is of the form (2) with $\varepsilon_1 = RC$.

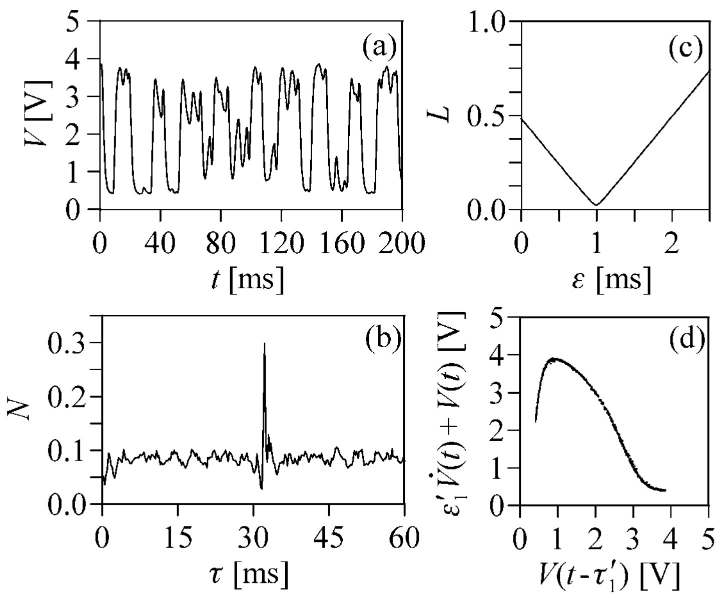

Figure 6. (a) Experimental time series of the electronic oscillator with delayed feedback. (b) Number N of pairs of extrema in the time series separated in time by τ, as a function of τ. $N(\tau)$ is normalized to the total number of extrema in the time series. $N_{\min}(\tau) = N(31.75\ \text{ms})$. (c) The $L(\varepsilon)$ plot. $L(\varepsilon)$ is normalized to the number of points. $L_{\min}(\varepsilon) = L(1.000\ \text{ms})$. (d) The recovered nonlinear function.

At $\tau_1 = 31.7$ ms and $\varepsilon_1 = 1.01$ ms we record the signal $V(t)$ [Fig. 6(a)] using an analog-to-digital converter with the sampling frequency $f_s = 4$ kHz. Since the delay time τ_1 is not a multiple of the sampling time $T_s = 0.25$ ms, the recovery of τ_1 cannot be absolutely accurate. For the step of τ variation equal to T_s, the absolute minimum of $N(\tau)$ takes place at $\tau_1' = 31.75$ ms [Fig. 6(b)]. The $L(\varepsilon)$ plot, constructed with τ_1' and the step of ε variation equal to 0.025 ms, demonstrates the minimum at $\varepsilon_1' = 1.000$ ms [Fig. 6(c)]. The recovered nonlinear function [Fig. 6(d)] coincides practically with the true transfer function of the amplifier.

Besides the $L(\varepsilon)$ plot we use two another criteria of quality for the system recovery. The first of them exploits synchronization of unidirectionally coupled time-delay systems. We try to synchronize the recovered model equation with the experimental system (9) applying the following synchronization scheme [27]:

$$\varepsilon_1' \dot{y}(t) = -y(t) + f'(y(t-\tau_1')) + k(V(t) - y(t)), \tag{10}$$

where $y(t)$ is the model variable, τ_1' and ε_1' are the recovered parameters, f' is the polynomial approximation of the reconstructed nonlinear function, and k is the coupling coefficient. If the recovered model parameters are close to the true ones and the coupling coefficient k is sufficiently large, the response system (10) rapidly synchronizes with the driving system (9). To quantify the measure of synchronization we calculate the synchronization error $\Delta = \langle |V(t) - y(t)| \rangle$, where $\langle \cdot \rangle$ denotes a time average.

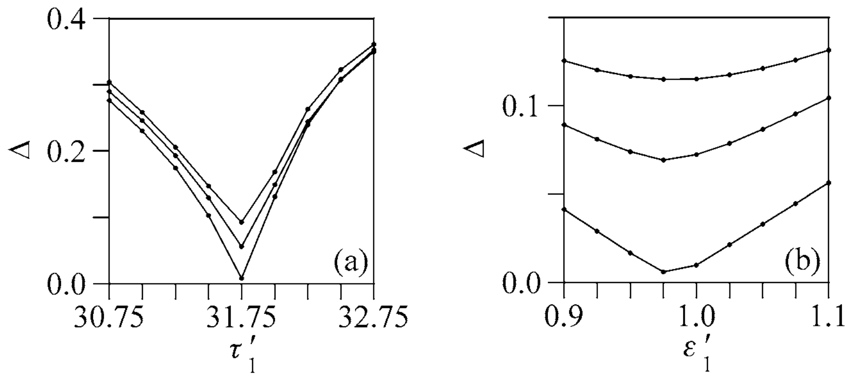

Figure 7. (a) Synchronization error Δ as a function of τ_1'. (b) Synchronization error Δ as a function of ε_1' From bottom to top, the curves refer to the additive noise level of 0%, 1% and 10%, respectively.

Figure 7(a) shows the dependence of Δ on the model parameter τ_1' varied in the vicinity of $\tau_1' = 31.75$ ms with the step of variation equal to T_s. To construct this plot we use $k = 0.5$, $\varepsilon_1' = 1.000$ ms, and approximation of the recovered function f' with a polynomial of degree 11. The value of Δ is computed after transients and is averaged over 2.5 s. The minimum of Δ is observed at $\tau_1' = 31.75$ ms as well as the minimum of $N(\tau)$. We also calculate the dependence of Δ on τ_1' after adding Gaussian white noise to the time series of the driving system. For the noise level of 1% and 10% the minimum of $\Delta(\tau_1')$ still takes place at $\tau_1' = 31.75$ ms [Fig. 7(a)]. Note that for the construction of $\Delta(\tau_1')$ in the presence of noise we use ε_1' and f' recovered from noisy time series.

In a similar way we plot the dependence of Δ on the model parameter ε_1' varied in the vicinity of $\varepsilon_1' = 1.000$ ms with the step of variation equal to 0.025 ms [Fig. 7(b)]. The minimum of $\Delta(\varepsilon_1')$ is observed at $\varepsilon_1' = 0.975$ ms which is slightly below the estimation of ε_1' obtained from the $L(\varepsilon)$ plot. This distinction between ε_1' estimations can result from inaccuracy of f' approximation performed for calculation of Δ. For the driving signal corrupted by additive Gaussian white noise of 1% and 10% the minimum of $\Delta(\varepsilon_1')$ is again observed at $\varepsilon_1' = 0.975$ ms [Fig. 7(b)]. As can be seen from Fig. 7, the inaccuracy of the delay time estimation gives a greater synchronization error than the inaccuracy of estimation of ε_1.

The next quantitative measure of accuracy used in this chapter for the recovered model is the one-step forecast error $\sigma = \left\langle \left| V(t) - y(t) \right| \right\rangle$, where $V(t)$ is the experimentally measured variable, $y(t)$ is the variable of the model having the form of Eq. (10) with $k = 0$, and $\left\langle \cdot \right\rangle$ denotes a time average. This measure shows how the model with the recovered τ_1', ε_1', and f' fits the observed data if the initial conditions for the one-step prediction are chosen from the experimental time series. The dependencies of σ on the parameters τ_1' and ε_1' are qualitatively similar to the dependencies $\Delta(\tau_1')$ and $\Delta(\varepsilon_1')$ (Fig. 7), respectively, and are not shown here.

4 Peculiarities of Ring Time-Delay System Reconstruction

In the ring time-delay systems described by Eq. (2) a dynamical variable can be measured at different points indicated in Fig. 2 by the numerals 1–3. However, it should be mentioned that in the real systems it is not always possible to localize the elements depicted in Fig. 2 or to choose the point of measurement because of the integrity of the system. The delayed feedback system recovery for the case when the observed dynamical variable is $x(t)$ measured at the point 1 has been considered in Sec. III.

In the case, when the observed dynamical variable is $x(t-\tau_1)$ measured at the point 2 (Fig. 2), one can use the same procedure for estimation of the system parameters as in the case of $x(t)$ measurement since the observable is simply shifted in time by the delay time τ_1 about $x(t)$. For example, reconstructing the electronic oscillator with delayed feedback described by Eq. (9) from experimental time series of voltage $V(t-\tau_1)$ at the delay line output we obtain the results qualitatively similar to those presented in Fig. 6 for the case of the system recovery from the time series of $V(t)$.

Let us consider a technique of the time-delay system (2) reconstruction for the third possible case, when the observed variable is $f(x(t-\tau_1))$ measured at the point 3 (Fig. 2). As well as in the time series of $x(t)$, there are practically no extrema separated in time by τ_1 in the time series of the variable $f(x(t-\tau_1))$, since $df(x(t-\tau_1))/dt = \left(df(x(t-\tau_1))/dx \right) \dot{x}(t-\tau_1)$. Then, the delay time τ_1 can be estimated by the location of the absolute minimum in the $N(\tau)$ plot constructed from the variable $f(x(t-\tau_1))$.

The nonlinear function f can be recovered by plotting $f(x(t-\tau_1))$ versus $x(t-\tau_1)$. To obtain the unknown values of $x(t-\tau_1)$ one has to filter the chaotic time series of the variable $f(x(t-\tau_1))$ with a low-frequency first-order filter with the cut-off frequency $\nu_1 = 1/\varepsilon_1$ and to shift the signal $x(t)$ at the filter output by the delay time τ_1 defined earlier. Since the parameter ε_1 and correspondingly the value of ν_1 are a priori unknown, we filter the time series of $f(x(t-\tau_1))$ under variation of the filter cut-off frequency $\nu = 1/\varepsilon$ and plot $f(x(t-\tau_1))$ versus $u(t-\tau_1)$, where $u(t-\tau_1)$ is the signal at the filter output shifted by the time τ_1. Note that a single-valued dependence in the plane $\left(u(t-\tau_1), f(x(t-\tau_1)) \right)$ is possible only for $\varepsilon = \varepsilon_1$. In this case $u(t-\tau_1) = x(t-\tau_1)$ and the set of points constructed in the plane reproduces the function *f*, which can be approximated if necessary. As a quantitative criterion of single-valuedness in searching for ε_1 we use again the minimal length of a line $L(\varepsilon)$ connecting all points in the plane $\big(u(t-\tau_1), f(x(t-\tau_1))\big)$ ordered with respect to $u(t-\tau_1)$. The minimum of $L(\varepsilon)$ is observed at $\varepsilon = \varepsilon_1$.

We apply the method to time series of the variable $f(x(t-\tau_1))$ of the Mackey-Glass equation [6]

$$\dot{x}(t) = -bx(1) + \frac{ax(t-\tau_1)}{1+x^c(t-\tau_1)}, \tag{11}$$

which can be converted to Eq. (2) by division by *b*. The parameters of the system (11) are chosen to be $a = 0.2$, $b = 0.1$, $c = 10$, and $\tau_1 = 300$ to produce a dynamics on a high-dimensional chaotic attractor [8]. Part of the time series is shown in Fig. 8(a). The location of the absolute minimum of $N(\tau)$ [Fig. 8(b)] allows us to recover the delay time, $\tau_1' = 300$. The step of τ variation in Fig. 8(b) is equal to the integration step $h = 1$. The minimum of $L(\varepsilon)$ [Fig. 8(c)] takes place at $\varepsilon_1' = 10.0$ ($\varepsilon_1 = 1/b = 10$). To construct the $L(\varepsilon)$ plot we use the step of ε variation equal to 0.1. The nonlinear function recovered using the estimated τ_1' and ε_1' [Fig. 8(d)] coincides practically with the true nonlinear function.

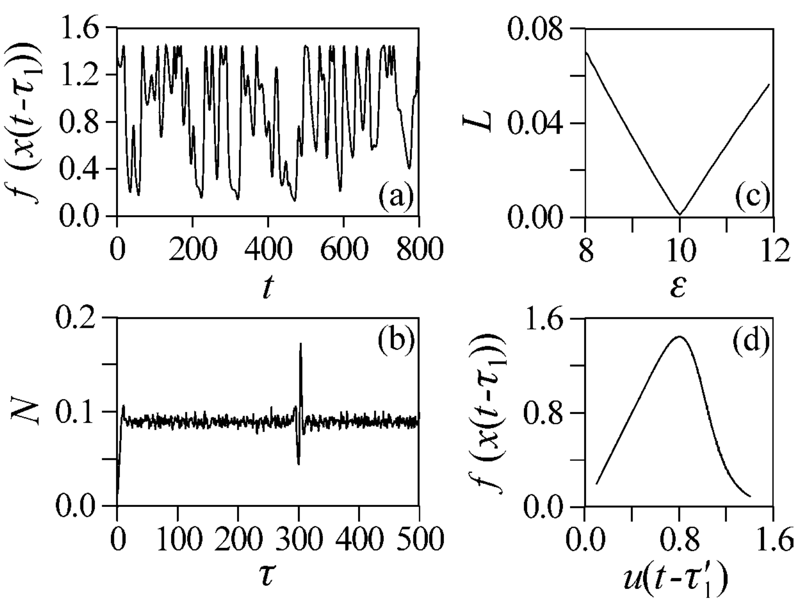

Figure 8. (a) The time series of the variable $f(x(t-\tau_1))$ of the Mackey-Glass system. (b) Number *N* of pairs of extrema in the time series of $f(x(t-\tau_1))$ separated in time by τ, as a function of τ. $N(\tau)$ is normalized to the total number of extrema in the time series. $N_{\min}(\tau) = N(300)$. (c) Length *L* of a line connecting points ordered with respect to $u(t-\tau_1')$ in the plane $\big(u(t-\tau_1'), f(x(t-\tau_1))\big)$, as a function of ε. $L(\varepsilon)$ is normalized to the number of points. $L_{\min}(\varepsilon) = L(10.0)$. (d) The recovered nonlinear function.

5 Reconstruction of Time-Delay Systems of High Order

The method of the delay time definition based on the statistical analysis of time intervals between extrema in the time series can be extended to time-delay systems of high order

$$\varepsilon_n x^{(n)}(t) + \varepsilon_{n-1} x^{(n-1)}(t) + \cdots + \varepsilon_1 \dot{x}(t) = F(x(t), x(t-\tau_1)). \tag{12}$$

Time differentiation of Eq. (12) gives

$$\varepsilon_n x^{(n+1)}(t) + \varepsilon_{n-1} x^{(n)}(t) + \cdots + \varepsilon_1 \ddot{x}(t) = \frac{\partial F(x(t), x(t-\tau_1))}{\partial x(t)} \dot{x}(t) + \frac{\partial F(x(t), x(t-\tau_1))}{\partial x(t-\tau_1)} \dot{x}(t-\tau_1). \tag{13}$$

For $\dot{x}(t) = 0$ the condition $\dot{x}(t-\tau_1) \neq 0$ will be satisfied if the left-hand side of Eq. (13) does not vanish. If a probability to obtain zero in the left-hand side of Eq. (13) is very small for the extremal points, the $N(\tau)$ plot qualitatively must have a shape similar to that inherent in the case of first-order delay-differential equations such as Eqs. (2) and (4).

We have found out that for sufficiently small values of ε_i, $i = 1, \ldots, n$, the $N(\tau)$ plot demonstrates the absolute minimum at $\tau = \tau_1$ as well in the case of the first-order time-delay systems. The distribution of the values of the left-hand side of Eq. (13) at the extremal points has a pronounced minimum in the neighborhood of zero in this case. As the parameters ε_i increase, the absolute minimum of $N(\tau)$ shifts from τ_1 to larger values. The greater are ε_i characterizing the influence of the system inertial elements, the greater is the shift. This time shift of $N(\tau)$ minimum does not depend on τ_1. Note that in the first-order time-delay systems the location of the absolute minimum in the $N(\tau)$ plot does not depend on ε_1.

The proposed method of the parameter ε_1 estimation and the nonlinear function recovery based on the projection of infinite-dimensional phase space of the time-delay system to suitably chosen two-dimensional subspaces can be also applied to a variety of time-delay systems of order higher than that of Eq. (2). For instance, if the dynamics of a time-delay system is governed by the second-order delay-differential equation

$$\varepsilon_2 \ddot{x}(t) + \varepsilon_1 \dot{x}(t) = -x(t) + f(x(t-\tau_1)), \tag{14}$$

the nonlinear function can be reconstructed by plotting in a plane a set of points with coordinates $\left(x(t-\tau_1), \varepsilon_2 \ddot{x}(t) + \varepsilon_1 \dot{x}(t) + x(t)\right)$. Since the parameters ε_1 and ε_2 are a priori unknown, one needs to plot $\hat{\varepsilon}_2 \ddot{x}(t) + \hat{\varepsilon}_1 \dot{x}(t) + x(t)$ versus $x(t-\tau_1)$ under variation of $\hat{\varepsilon}_1$ and $\hat{\varepsilon}_2$, searching for a single-valued dependence, which is possible only for $\hat{\varepsilon}_1 = \varepsilon_1$, $\hat{\varepsilon}_2 = \varepsilon_2$. In this search for ε_1 and ε_2 we calculate the length of a line $L(\hat{\varepsilon}_1, \hat{\varepsilon}_2)$ connecting points ordered with respect to $x(t-\tau_1)$ in the plane $\left(x(t-\tau_1), \hat{\varepsilon}_2 \ddot{x}(t) + \hat{\varepsilon}_1 \dot{x}(t) + x(t)\right)$. The minimum of $L(\hat{\varepsilon}_1, \hat{\varepsilon}_2)$ is observed at $\hat{\varepsilon}_1 = \varepsilon_1$, $\hat{\varepsilon}_2 = \varepsilon_2$. The set of points constructed in the plane for these defined values of ε_1 and ε_2 reproduces the nonlinear function.

The methods of reconstruction of second-order time-delay systems from scalar time series have been considered in Refs. [10, 17, 18]. However, these methods deal only with the recovery of the delay time and the nonlinear function. For the recovery of the latter one they use only the points of the phase space section. As the result, these methods need long time series for qualitative reconstruction of the nonlinear function. The proposed by us procedure of the delay time estimation based on the statistical analysis of time intervals between extrema in the time series needs significantly smaller time of computation than the methods of the delay time definition based on calculation of the filling factor of the projected time series [17] and minimization of the one-step forecast error of the recovered model equation [10, 18].

To verify the method efficiency we have applied it to experimental time series gained from the electronic oscillator with delayed feedback that is similar to that considered in Sec. III, but contains two identical low-frequency in-series *RC*-filters. The dynamics of this oscillator is governed by Eq. (14), where $x(t)$ and $x(t-\tau_1)$ are the delay line input and output voltages, respectively, $\varepsilon_1 = R_1C_1 + R_2C_2$, and $\varepsilon_2 = R_1C_1R_2C_2$, where R_1, R_2, C_1, and C_2 are, respectively, the resistances and capacitances of the first and the second filters.

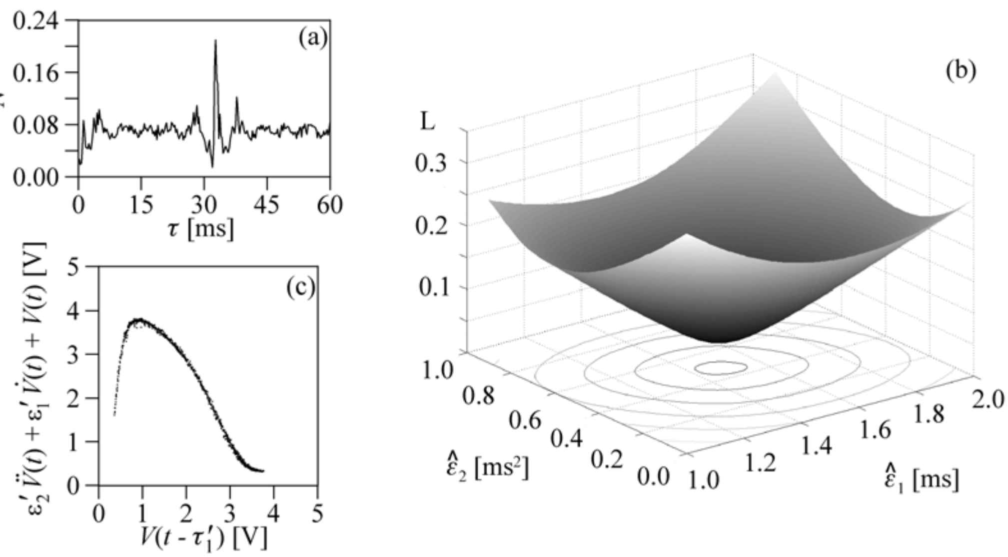

Figure 9. Reconstruction of the electronic oscillator with delayed feedback with a two-section filter. (a) Number N of pairs of extrema in the experimental time series separated in time by τ normalized to the total number of extrema. $N_{\min}(\tau) = N(31.75\ \text{ms})$. (b) The $L(\hat{\varepsilon}_1,\ \hat{\varepsilon}_2)$ plot normalized to the number of points. $L_{\min}(\hat{\varepsilon}_1,\ \hat{\varepsilon}_2) = L(1.48\ \text{ms},\ 0.48\ \text{ms}^2)$. (c) The recovered nonlinear function.

Using the analog-to-digital converter we record with the sampling frequency $f_s = 4$ kHz the time series of voltage at the delay line input for $\tau_1 = 31.7$ ms, $R_1C_1 = 1.01$ ms, and $R_2C_2 = 0.48$ ms ($\varepsilon_1 = 1.49$ ms and $\varepsilon_2 = 0.48$ ms^2). The absolute minimum of $N(\tau)$ is observed at $\tau_1' = 31.75$ ms [Fig. 9(a)]. The $L(\hat{\varepsilon}_1,\ \hat{\varepsilon}_2)$ plot, constructed with the step of $\hat{\varepsilon}_1$ variation equal to 0.01 ms and the step of $\hat{\varepsilon}_2$ variation equal to 0.01 ms^2, demonstrates the minimum at $\varepsilon_1' = 1.48$ ms and $\varepsilon_2' = 0.48$ ms^2 [Fig. 9(b)]. These ε_1' and ε_2' values give the following estimation of the filter parameters: $(R_1C_1)' = 1.00$ ms and $(R_2C_2)' = 0.48$ ms. The recovered nonlinear function [Fig. 9(c)] coincides with a good accuracy with the true transfer function of the nonlinear element.

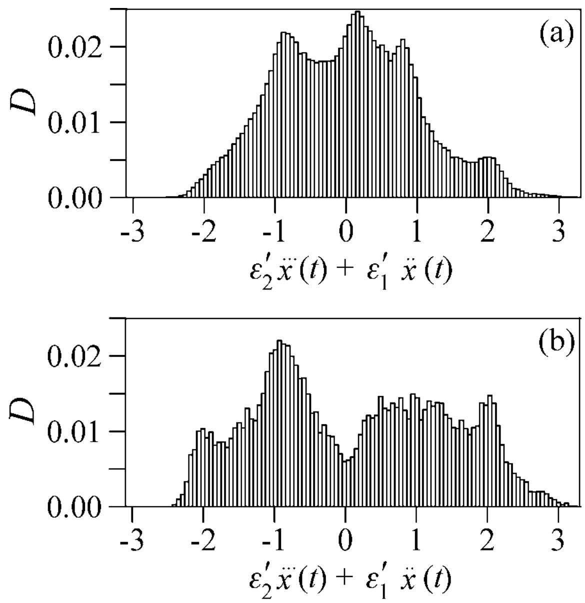

Figure 10. Distribution D of the sum $\varepsilon_2'\dddot{x}(t)+\varepsilon_1'\ddot{x}(t)$ for all points of the experimental time series (a) and for the extremal points (b).

With the recovered parameters ε_1' and ε_2' we plot the distribution of the sum $\varepsilon_2'\dddot{x}(t)+\varepsilon_1'\ddot{x}(t)$ using all points of the time series [Fig. 10(a)]. The maximum of this distribution is observed close to zero. The distribution of the same sum constructed using only the extremal points $\dot{x}(t)=0$ demonstrates a pronounced minimum in the vicinity of zero [Fig. 10(b)]. This result counts in favor of the conclusion that the probability to obtain zero in the left-hand side of Eq. (13) is sufficiently small at the extremal points. The presence of minimum in the vicinity of zero in Fig. 10(b) agrees well with the existence of minimum at the delay time of the system in the $N(\tau)$ plot [Fig. 9(a)].

The next example is the method application to time series of the third-order time-delay system

$$\varepsilon_3\dddot{x}(t)+\varepsilon_2\ddot{x}(t)+\varepsilon_1\dot{x}(t)=-x(t)+f(x(t-\tau_1)) \tag{15}$$

with quadratic nonlinear function $f(x)=\lambda-x^2$, where λ is the parameter of nonlinearity. The parameters of the system (15) are chosen to be $\tau_1=300$, $\lambda=1.9$, $\varepsilon_1=4$, $\varepsilon_2=5$, and $\varepsilon_3=2$. The $N(\tau)$ plot, constructed with the step of τ variation equal to unity, shows the absolute minimum at $\tau_1'=301$ [Fig. 11(a)]. The minimum of $N(\tau)$ tends to $\tau_1=300$ as the parameters ε_i decrease and shifts to larger τ as ε_i increase. For example, we obtain $\tau_1'=300$ at $\varepsilon_1=2.5$, $\varepsilon_2=2$, and $\varepsilon_3=0.5$ and $\tau_1'=302$ at $\varepsilon_1=8$, $\varepsilon_2=17$, and $\varepsilon_3=10$. The higher is the order of the time-delay system (12), the more parameters are to be fitted. This problem is typical in high-dimensional search space. As the result, the time of computation significantly increases. Since our procedure of the parameters estimation involves numerical calculation of the derivatives, the quality of reconstruction deteriorates with the increase of the time-delay system order, resulting in the necessity to calculate more high-order derivatives. In Fig. 11(b) the recovered nonlinear function of Eq. (15) is shown. The quality of this function recovery is worse than the quality of reconstruction for the first-order time-delay systems (8) and (11) [Figs. 4 and 8].

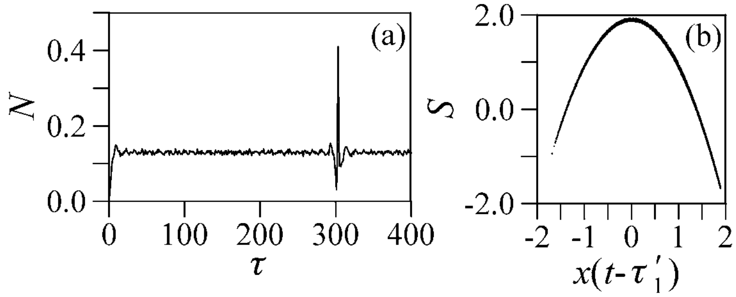

Figure 11. (a) Number N of pairs of extrema in the time series of Eq. (15) separated in time by τ, as a function of τ. $N(\tau)$ is normalized to the total number of extrema in the time series. $N_{\min}(\tau) = N(301)$. (b) The recovered nonlinear function. $S = \varepsilon_3' \dddot{x}(t) + \varepsilon_2' \ddot{x}(t) + \varepsilon_1' \dot{x}(t) + x(t)$.

Since the considered method of the delay time definition provides accurate estimation of τ_1 for high-order time-delay systems only at small ε_i values, we modify the method in order to achieve exact recovery of τ_1 for any values of the parameters ε_i. Let us consider the modified method with the second-order delay-differential equation (14) as an example. Differentiating Eq. (14) with respect to time, we obtain

$$\varepsilon_2 \dddot{x}(t) + \varepsilon_1 \ddot{x}(t) = -\dot{x}(t) + \frac{df(x(t-\tau_1))}{dx(t-\tau_1)} \dot{x}(t-\tau_1) . \tag{16}$$

Let us also construct the $N(\tau)$ plot, but, instead of using all extrema of time series as in the case of first-order time-delay systems, we will select only the points of extrema $\dot{x}(t) = 0$ at which the second and the third derivatives ($\ddot{x}(t)$ and $\dddot{x}(t)$) have the same sign. As can be seen from Eq. (16), for such points with $\dot{x}(t) = 0$ the condition $\dot{x}(t-\tau_1) \neq 0$ must be fulfilled at positive ε_1 and ε_2. Thus, there must be no extremum separated in time by τ_1 from the given one and, hence, $N(\tau_1) \to 0$.

This modified method of determination of the delay time can also be used with time-delay systems of higher orders. In such cases, the $N(\tau)$ plots should be constructed using only extrema in which all high-order derivatives $x^{(n)}(t)$, $n = 2, \ldots, k+1$, (where k is the order of equation) have the same sign. However, as the order of the system increases, realization of this approach requires longer time series and the accuracy of τ_1 determination decreases as a result of increasing inaccuracy of the numerical evaluation of high-order derivatives.

6 Determining Order of a Time-Delay System

The modified method of reconstruction of high-order time-delay systems considered in Sec. V can be used for evaluating the a priori unknown order of a system from its time series.

The idea of this approach consists in reconstructing the given system assuming that it is described by a time-delay equation of the first order, then reconstructing it as a time-delay system of the second order, and so on. A criterion of correct determination of the order of a model differential equation can be formulated in terms of the single-valuedness of a reconstructed nonlinear function. A quantitative measure of this single-valuedness can be the minimum length L of the line connecting points on the plot of the reconstructed nonlinear function.

Let us consider a time series generated by the time-delay system of the first order

$$\varepsilon_1 \dot{x}(t) = -x(t) + f(x(t-\tau_1)) \tag{17}$$

with the quadratic nonlinear function $f(x) = \lambda - x^2$ and the parameters $\tau_1 = 1000$, $\lambda = 1.95$, and $\varepsilon_1 = 25$. We imagine that the order of the system is a priori unknown. First, we reconstruct a model equation assuming that the system is of the first order and has the form of Eq. (17). To recover the delay time we construct the $N(\tau)$ plot using all extrema of the time series. For the step of τ variation equal to 10, the absolute minimum of $N(\tau)$ takes place at $\tau_1' = 1000$ [Fig. 12(a)]. In order to recover the parameter ε_1 we plot $\hat{\varepsilon}_1 \dot{x}(t) + x(t)$ versus $x(t-\tau_1')$ under variation of $\hat{\varepsilon}_1$ and calculate the length $L(\hat{\varepsilon}_1)$ of the line connecting points in the plane $\left(x(t-\tau_1'),\ \hat{\varepsilon}_1 \dot{x}(t) + x(t)\right)$, which are ordered with respect to $x(t-\tau_1')$. For $\hat{\varepsilon}_1$ varied at the step of unity, the $L(\hat{\varepsilon}_1)$ plot exhibits the minimum $L_{\min}(\hat{\varepsilon}_1) = 0.009$ at $\varepsilon_1' = 25$ [Fig. 12(b)]. The reconstructed nonlinear function is presented in Fig. 12(c).

Reconstructing the model equation of the system as the second-order equation of type (14), we use the modified method of delay time recovery described above. Varying τ and counting for various τ the number N of cases where $\dot{x}(t)$ and $\dot{x}(t-\tau)$ simultaneously vanish and $\ddot{x}(t)$ and $\ddot{x}(t)$ have the same sign, we have plotted $N(\tau)$ [Fig. 12(d)]. In this figure the dependence $N(\tau)$ is normalized to the number of extrema in the time series where $\ddot{x}(t)$ and $\ddot{x}(t)$ have the same sign. The derivatives are calculated using a local polynomial approximation. The $N(\tau)$ plot, constructed by this method with the step of τ variation equal to 10, yields the estimation $\tau_1' = 990$ [Fig. 12(d)]. For this delay time the $L(\hat{\varepsilon}_1,\ \hat{\varepsilon}_2)$ plot, constructed with the step of $\hat{\varepsilon}_1$ variation equal to 0.5 and the step of $\hat{\varepsilon}_2$ variation equal to 5, demonstrates the minimum $L_{\min}(\hat{\varepsilon}_1,\ \hat{\varepsilon}_2) = 0.047$ at $\varepsilon_1' = 32$ and $\varepsilon_2' = 335$ [Fig. 12(e)]. The nonlinear function reconstructed for these parameters is presented in Fig. 12(f). The quality of the nonlinear function recovery in Fig. 12(c) is much better than that in Fig. 12(f), and the minimum $L_{\min}(\hat{\varepsilon}_1)$ is five times smaller than $L_{\min}(\hat{\varepsilon}_1,\ \hat{\varepsilon}_2)$. The obtained results clearly indicate that the true model system is described by the first-order equation. It should be noted that in the case of exact recovery of the delay time τ_1 by the modified method, the minimum of $L(\hat{\varepsilon}_1,\ \hat{\varepsilon}_2)$ is observed at $\varepsilon_1' = 25$ and $\varepsilon_2' = 0$, which also indicates that the model system is of the first order. In this case $L_{\min}(\hat{\varepsilon}_1,\ \hat{\varepsilon}_2) = L_{\min}(\hat{\varepsilon}_1) = 0.009$ and the reconstructed nonlinear function coincides with that depicted in Fig. 12(c).

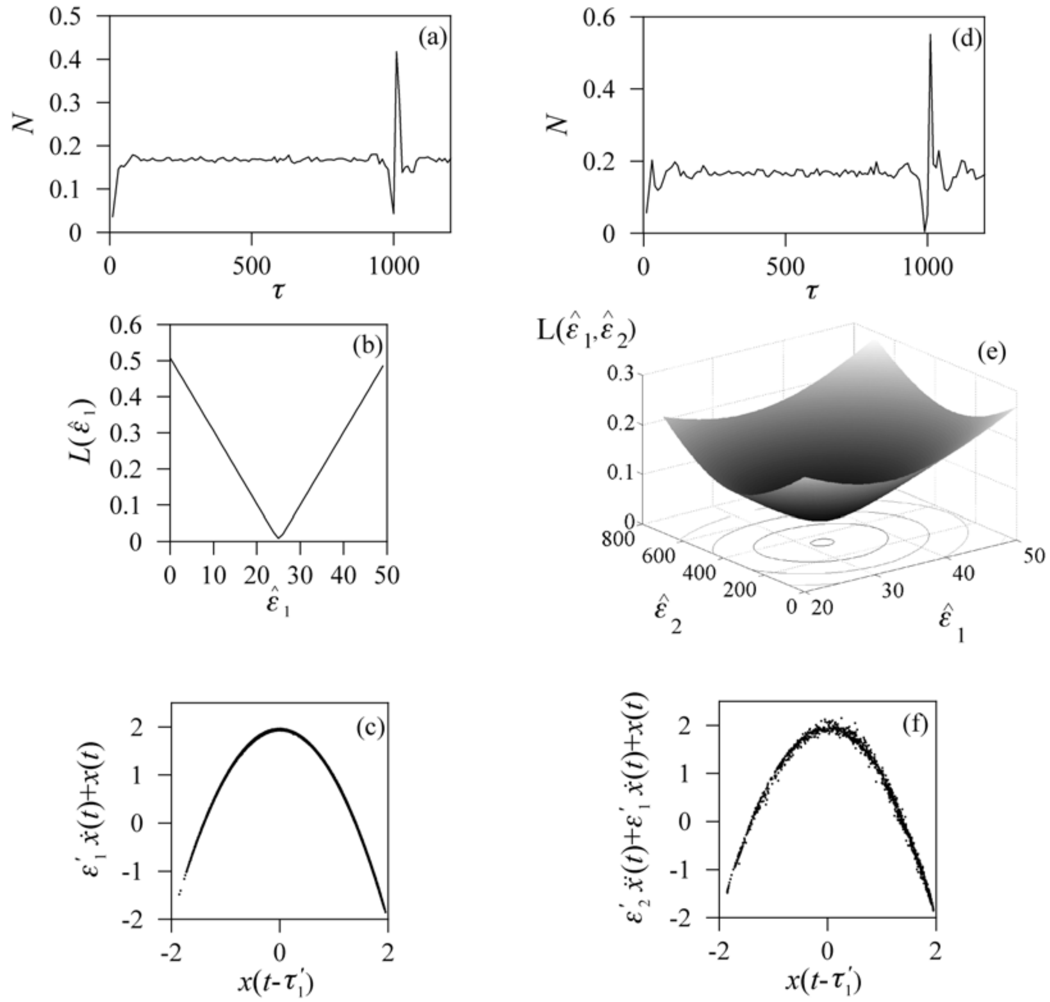

Figure 12. Reconstruction of the first-order time-delay system (17). (a) The $N(\tau)$ plot constructed using all extrema of the time series. $N_{\min}(\tau)=N(1000)$. (b) The $L(\hat{\varepsilon}_1)$ plot constructed for $\tau'_1=1000$. $L_{\min}(\hat{\varepsilon}_1)=L(25)=0.009$. (c) The recovered nonlinear function for $\tau'_1=1000$ and $\varepsilon'_1=25$. (d) The $N(\tau)$ lot constructed using the modified method. $N_{\min}(\tau)=N(990)$. (e) The $L(\hat{\varepsilon}_1,\,\hat{\varepsilon}_2)$ plot constructed for $\tau'_1=990$. $L_{\min}(\hat{\varepsilon}_1,\,\hat{\varepsilon}_2)=L(32,\;335)=0.047$. (f) The recovered nonlinear function for $\tau'_1=990$, $\varepsilon'_1=32$, and $\varepsilon'_2=335$.

Now let us consider a situation where the time series is generated by the second-order time-delay system (14) with the quadratic nonlinear function and the parameters $\tau_1=1000$, $\lambda=1.95$, $\varepsilon_1=45$, and $\varepsilon_2=500$. Reconstructing the model equation under the assumption that the system is described by the first-order Eq. (17), we obtain the following results. For the step of τ variation equal to 10, the minimum of $N(\tau)$ is observed at $\tau'_1=1010$ [Fig. 13(a)]. For $\hat{\varepsilon}_1$ varied at the step of unity, the $L(\hat{\varepsilon}_1)$ plot demonstrates the minimum at $\varepsilon'_1=39$ [Fig. 13(b)]. The recovered nonlinear function is shown in Fig. 13(c).

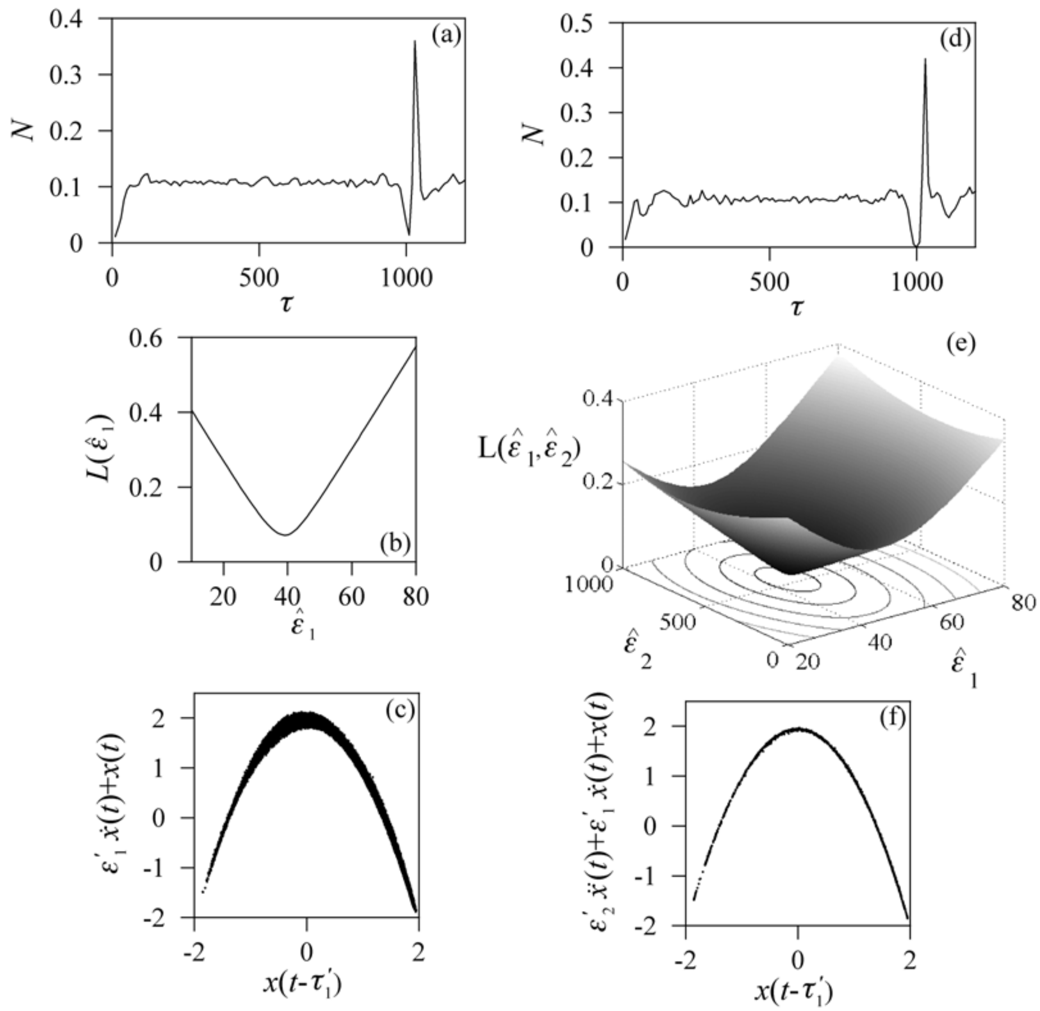

Figure 13. Reconstruction of the second-order time-delay system (14). (a) The $N(\tau)$ plot constructed using all extrema of the time series. $N_{\min}(\tau) = N(1010)$. (b) The $L(\hat{\varepsilon}_1)$ plot constructed for $\tau_1' = 1010$. $L_{\min}(\hat{\varepsilon}_1) = L(39) = 0.072$. (c) The recovered nonlinear function for $\tau_1' = 1010$ and $\varepsilon_1' = 39$. (d) The $N(\tau)$ plot constructed using the modified method. $N_{\min}(\tau) = N(1000)$. (e) The $L(\hat{\varepsilon}_1,\ \hat{\varepsilon}_2)$ plot constructed for $\tau_1' = 1000$. $L_{\min}(\hat{\varepsilon}_1,\ \hat{\varepsilon}_2) = L(44.5,\ 540) = 0.012$. (f) The recovered nonlinear function for $\tau_1' = 1000$, $\varepsilon_1' = 44.5$, and $\varepsilon_2' = 540$.

These results have to be compared with those obtained upon reconstruction of the system assuming that it is described by the second-order equation. The $N(\tau)$ plot constructed by the modified method demonstrates the absolute minimum at $\tau = \tau_1 = 1000$ [Fig. 13(d)]. The $L(\hat{\varepsilon}_1,\ \hat{\varepsilon}_2)$ plot, constructed with the step of $\hat{\varepsilon}_1$ variation equal to 0.5 and the step of $\hat{\varepsilon}_2$ variation equal to 5, exhibits the minimum at $\varepsilon_1' = 44.5$ and $\varepsilon_2' = 540$ [Fig. 13(e)]. The nonlinear function reconstructed for these values [Fig. 13(f)] coincides quite well with the true quadratic function of the system. As can be seen, the quality of reconstruction of the nonlinear function is much better in Fig. 13(f) than in Fig. 13(c), and the minimum $L_{\min}(\hat{\varepsilon}_1,\ \hat{\varepsilon}_2) = L(44.5,\ 540) = 0.012$ in Fig. 13(e) is six times smaller than $L_{\min}(\hat{\varepsilon}_1) = L(39) = 0.072$ in Fig. 13(b). This comparison indicates that the system under investigation is better described by the second-order equation.

7 Recovery of Time-Delay Systems with Two Coexisting Delays

Let us consider now a time-delay system with two different delay times τ_1 and τ_2

$$\dot{x}(t) = F(x(t), x(t-\tau_1), x(t-\tau_2)) . \tag{18}$$

Differentiation of Eq. (18) with respect to *t* gives

$$\ddot{x}(t) = \frac{\partial F}{\partial x(t)}\dot{x}(t) + \frac{\partial F}{\partial x(t-\tau_1)}\dot{x}(t-\tau_1) + \frac{\partial F}{\partial x(t-\tau_2)}\dot{x}(t-\tau_2) . \tag{19}$$

Similarly to temporal realization of Eq. (4), the realization $x(t)$ of Eq. (18) has mainly quadratic extrema and therefore $\dot{x}(t) = 0$ and $\ddot{x}(t) \neq 0$ at the extremal points. Hence, if $\dot{x}(t) = 0$, the condition

$$a\dot{x}(t-\tau_1) + b\dot{x}(t-\tau_2) \neq 0 \tag{20}$$

must be fulfilled, where $a = \partial F(x(t), x(t-\tau_1), x(t-\tau_2)) / \partial x(t-\tau_1)$ and $b = \partial F(x(t), x(t-\tau_1), x(t-\tau_2)) / \partial x(t-\tau_2)$. The condition (20) can be satisfied only if $\dot{x}(t-\tau_1) \neq 0$ or/and $\dot{x}(t-\tau_2) \neq 0$. By this is meant that the derivatives $\dot{x}(t)$ and $\dot{x}(t-\tau_1)$, or $\dot{x}(t)$ and $\dot{x}(t-\tau_2)$ do not vanish simultaneously. As the result, the number of extrema separated in time by τ_1 and τ_2 from a quadratic extremum must be appreciably less than the number of extrema separated in time by other values of τ and hence, the $N(\tau)$ plot will demonstrate pronounced minima at $\tau = \tau_1$ and $\tau = \tau_2$. Compared to the method of optimal transformations used in Ref. [19] for the recovery of two delays our method requires longer time series, but it is significantly more simple and does not need preprocessing of the data as for example, adaptive partitioning of data used in Ref. [19].

We illustrate the procedure for estimating the other characteristics of time-delay system with two delays from time series for the system governed by the following equation

$$\varepsilon_1\dot{x}(t) = -x(t) + f_1(x(t-\tau_1)) + f_2(x(t-\tau_2)) . \tag{21}$$

Differentiation of Eq. (21) with respect to *t* gives

$$\varepsilon_1\ddot{x}(t) = -\dot{x}(t) + \frac{\partial f_1(x(t-\tau_1))}{\partial x(t-\tau_1)}\dot{x}(t-\tau_1) + \frac{\partial f_2(x(t-\tau_2))}{\partial x(t-\tau_2)}\dot{x}(t-\tau_2) . \tag{22}$$

From Eq. (22) it follows that if

$$\dot{x}(t-\tau_1) = \dot{x}(t-\tau_2) = 0 , \tag{23}$$

then $\varepsilon_1\ddot{x}(t) = -\dot{x}(t)$ and

$$\varepsilon_1 = -\frac{\dot{x}(t)}{\ddot{x}(t)} . \tag{24}$$

Thus, to estimate the parameter ε_1 one can find the points of $x(t)$ satisfying condition (23), define for them the first and the second derivatives, calculate ε_1 using Eq. (24), and conduct averaging. Note that one can also use Eq. (24) for the recovery of ε_1 in the case of a single delay, but such estimation uses only the points with $\dot{x}(t-\tau_1)=0$ and is not so accurate as the method considered in Sec. III. To reduce the computation time we use Eq. (24) for the first approximation of the parameter ε_1 and improve this estimation later on.

To recover the nonlinear functions f_1 and f_2 we project the trajectory generated by Eq. (21) to a three-dimensional space $\left(x(t-\tau_1), x(t-\tau_2), \varepsilon_1\dot{x}(t)+x(t)\right)$. In this space the projected trajectory is confined to a two-dimensional surface since according to Eq. (21)

$$\varepsilon_1\dot{x}(t)+x(t)=f_1(x(t-\tau_1))+f_2(x(t-\tau_2)). \tag{25}$$

The section of this surface with the $x(t-\tau_2)=\text{const}$ plane enables one to recover the nonlinear function f_1 up to a constant since the points of the section are correlated via $\varepsilon_1\dot{x}(t)+x(t)=f_1(x(t-\tau_1))+c_1$, where $c_1=f_2(x(t-\tau_2))$ for some fixed value of $x(t-\tau_2)$. In a similar way one can recover up to a constant the nonlinear function f_2 by intersecting the trajectory projected to the above-mentioned three-dimensional space with the $x(t-\tau_1)=\text{const}$ plane. The points of this section are correlated via $\varepsilon_1\dot{x}(t)+x(t)=f_2(x(t-\tau_2))+c_2$, where $c_2=f_1(x(t-\tau_1))$ for fixed $x(t-\tau_1)$.

We demonstrate the method efficiency with a generalized Mackey-Glass equation obtained by introducing a further delay,

$$\dot{x}(t)=-bx(t)+\frac{1}{2}\frac{a_1x(t-\tau_1)}{1+x^c(t-\tau_1)}+\frac{1}{2}\frac{a_2x(t-\tau_2)}{1+x^c(t-\tau_2)}. \tag{26}$$

Division of Eq. (26) by b reduces it to Eq. (21) with $\varepsilon_1=1/b$. Figure 14(a) shows the $N(\tau)$ plot for $a_1=0.2$, $a_2=0.3$, $b=0.1$, $c=10$, $\tau_1=70$, and $\tau_2=300$. The first two most pronounced minima of $N(\tau)$ are observed at $\tau_1'=69$ and $\tau_2'=300$. Another distinctive minimum of $N(\tau)$ is observed close to $\tau=\tau_1+\tau_2$. Processing the points satisfying condition (23) with the recovered values τ_1' and τ_2' we obtain the averaged estimation $\varepsilon_1'=9.4$ for the parameter $\varepsilon_1=1/b=10$. To reduce inaccuracy in ε_1 determination by formula (24) we exclude from consideration the points with very small values of $\ddot{x}(t)$.

Projecting the time series of Eq. (26) to the three-dimensional space $\left(x(t-\tau_1'), x(t-\tau_2'), \varepsilon_1'\dot{x}(t)+x(t)\right)$ and constructing the sections of this space with the planes $x(t-\tau_2')=\text{const}$ and $x(t-\tau_1')=\text{const}$ we obtain at these sections the recovered nonlinear functions f_1 and f_2 [Figs. 14(b) and (c)]. However, as the result of inaccuracy in estimation of τ_1 and ε_1 the quality of the nonlinear function recovery is not good enough.

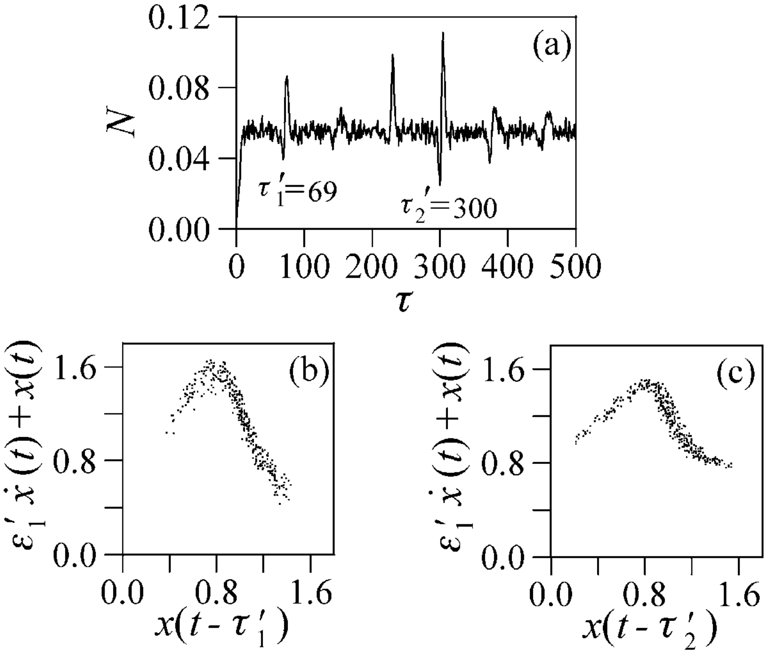

Figure 14. (a) Number N of pairs of extrema in the time series of Eq. (26) separated in time by τ, as a function of τ. $N(\tau)$ is normalized to the total number of extrema in the time series. (b) The recovered nonlinear function f_1. (c) The recovered nonlinear function f_2.

To achieve more high quality of the model equation reconstruction we propose the following procedure for the correction of the parameters. Varying τ_1 in a small vicinity of $\tau_1' = 69$ we project the time series to several three-dimensional $\left(x(t-\tau_1), x(t-\tau_2'), \varepsilon_1'\dot{x}(t)+x(t)\right)$ spaces and plot their sections with the $x(t-\tau_2') = \text{const}$ plane, searching for a section, which points contract to a curve demonstrating almost single-valued dependence. As a quantitative criterion of single-valuedness we use the minimal length of a line $L(\tau_1)$ connecting all points of the section ordered with respect to abscissa. The $L(\tau_1)$ plot demonstrates the minimum at $\hat{\tau}_1 = 70$ [Fig. 15(a)]. Similarly, the correction of the delay time τ_2 is performed. We project the time series to $\left(x(t-\hat{\tau}_1),\ x(t-\tau_2),\ \varepsilon_1'\dot{x}(t)+x(t)\right)$ spaces under variation of τ_2 in the vicinity of $\tau_2' = 300$ and plot the sections $x(t-\hat{\tau}_1) = \text{const}$. Note that for these sections the corrected delay time $\hat{\tau}_1 = 70$ is used. The minimum of $L(\tau_2)$ takes place at $\hat{\tau}_2 = 300$ [Fig. 15(b)]. In the general case if $\hat{\tau}_2 \neq \tau_2'$, the procedure of τ_1 revision is repeated by plotting the sections of the embedding spaces with the $x(t-\hat{\tau}_2) = \text{const}$ plane with the corrected delay time $\hat{\tau}_2$. Successive correction of τ_1 and τ_2 is continued until the parameters cease changing. For small deviations of initial estimates τ_1' and τ_2' from the true delay times the procedure is converging and allows one to define both delay times accurately.

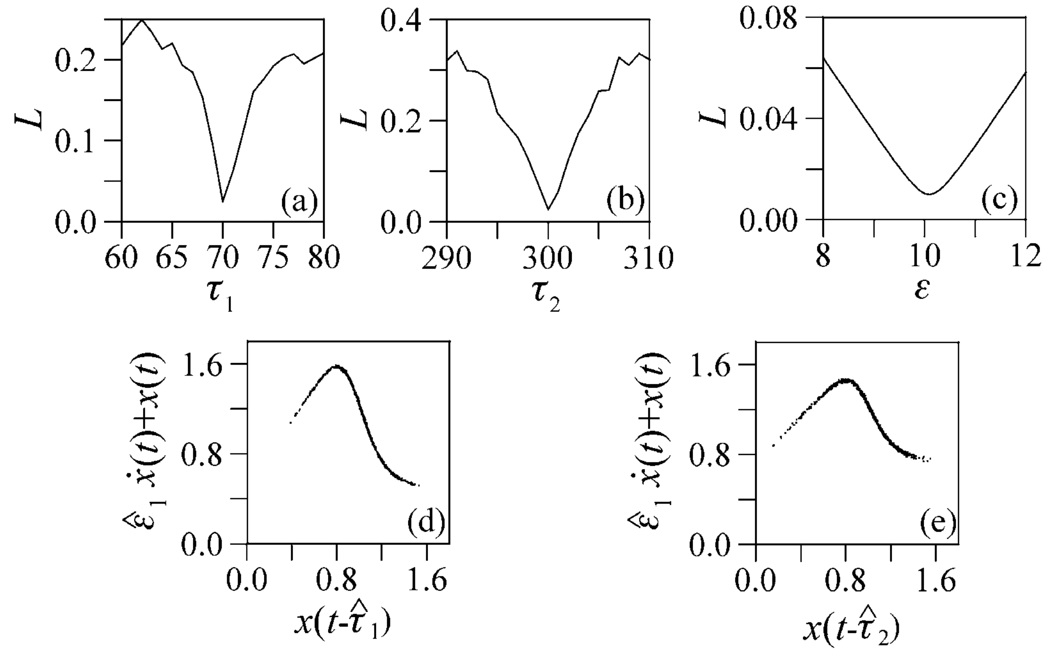

Figure 15. (a) Length L of a line connecting points ordered with respect to abscissa in the $x(t-\tau_2')=1$ section, as a function of τ_1. $L_{\min}(\tau_1)=L(70)$. (b) Length L of a line connecting points ordered with respect to abscissa in the $x(t-\hat{\tau}_1)=1$ section, as a function of τ_2. $L_{\min}(\tau_2)=L(300)$. (c) Length L of a line connecting points ordered with respect to abscissa in the $x(t-\hat{\tau}_2)=1$ section, as a function of ε. $L_{\min}(\varepsilon)=L(10.1)$. (d) Nonlinear function f_1 recovered up to the constant $\hat{c}_1=f_2(x(t-\hat{\tau}_2))$, where $x(t-\hat{\tau}_2)=1$. (e) Nonlinear function f_2 recovered up to the constant $\hat{c}_2=f_1(x(t-\hat{\tau}_1))$, where $x(t-\hat{\tau}_1)=1$.

After revision of the delay times the parameter ε_1 should be corrected. Its new estimate $\hat{\varepsilon}_1$ can be obtained by formula (24). However, a more reliable estimation is the one using all points of one of the section. To obtain it we project the time series to $\left(x(t-\hat{\tau}_1),\ x(t-\hat{\tau}_2),\ \varepsilon\dot{x}(t)+x(t)\right)$ spaces under variation of ε in the vicinity of ε_1', searching for a single-valued dependence in the section $x(t-\hat{\tau}_1)=\text{const}$ or in the section $x(t-\hat{\tau}_2)=\text{const}$. The $L(\varepsilon)$ plot shows the minimum at $\hat{\varepsilon}_1=10.1$ [Fig. 15(c)]. In Fig. 15 the values of $L(\varepsilon)$, $L(\tau_1)$, and $L(\tau_2)$ are normalized to the number of points in the corresponding section. Note that the proposed procedure of the successive correction of the parameters needs in several orders of magnitude smaller time of computation than the method of simultaneous selection of the parameters ε_1, τ_1, and τ_2 for the three-dimensional embedding space $\left(x(t-\tau_1), x(t-\tau_2), \varepsilon\dot{x}(t)+x(t)\right)$.

Figures 15(d) and (e) illustrate the reconstructed nonlinear functions of the system with two coexisting delays (26) for the corrected parameters $\hat{\varepsilon}_1=10.1$, $\hat{\tau}_1=70$, and $\hat{\tau}_2=300$. The nonlinear functions f_1 and f_2 are recovered up to the constant by plotting the sections of the two-dimensional surface described by Eq. (25). To investigate the method efficiency in the presence of noise we apply it to noisy data and found that the method provides sufficiently accurate reconstruction of the investigated system for noise levels up to 10% (the signal-to-noise ratio is 20 dB).

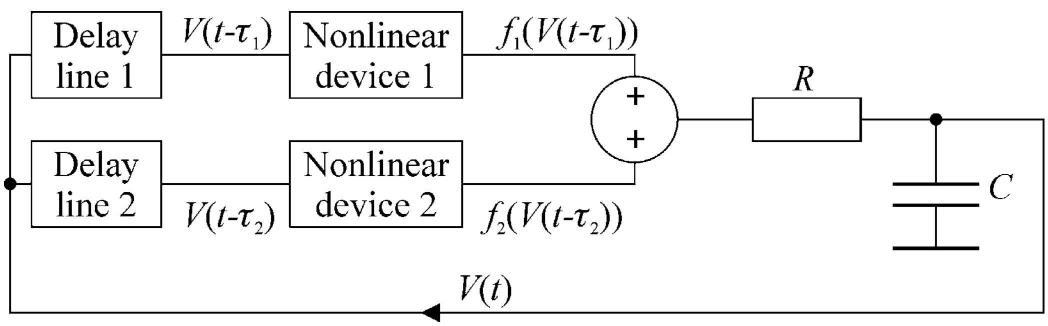

Figure 16. Block diagram of the electronic oscillator with two delays.

As another example, we consider the method application to experimental time series produced by a setup with two delays. A block diagram of the electronic scheme is shown in Fig. 16. This electronic oscillator is governed by Eq. (25), where $x(t)$ is the voltage at the input of the delay lines, $x(t-\tau_1)$ and $x(t-\tau_2)$ are the output voltages of the first and the second delay lines, respectively, and $\varepsilon_1 = RC$. The time series of $V(t)$ are recorded at $\tau_1 = 23.0$ ms, $\tau_2 = 31.1$ ms, and $\varepsilon_1 = 1.01$ ms with the sampling frequency $f_s = 4$ kHz. The $N(\tau)$ plot, constructed with the step of τ variation equal to the sampling time $T_s = 0.25$ ms, demonstrates the first two most pronounced minima at $\tau_1' = 23.0$ ms and $\tau_2' = 31.0$ ms [Fig. 17(a)]. These values of the delay times allow us to obtain the estimation $\varepsilon_1' = 1.16$ ms from Eqs. (23) and (24). To obtain the estimation of ε_1 using more number of points we project the time series to $\left(V(t-\tau_1'),\ V(t-\tau_2'),\ \varepsilon\dot{V}(t)+V(t)\right)$ spaces under variation of ε in the vicinity of ε_1', searching for a single-valued dependence in the section $V(t-\tau_1') = \text{const}$. The $L(\varepsilon)$ plot, constructed with the step of ε variation equal to 0.01 ms, demonstrates the minimum at $\hat{\varepsilon}_1 = 1.01$ ms [Fig. 17(b)]. The recovered nonlinear functions f_1 and f_2 are presented in Figs. 17(c) and (d), respectively, for $\tau_1' = 23.0$ ms, $\tau_2' = 31.0$ ms, and $\hat{\varepsilon}_1 = 1.01$ ms. These functions are recovered up to a constant and are sufficiently close to the true transfer functions of the nonlinear elements of the scheme.

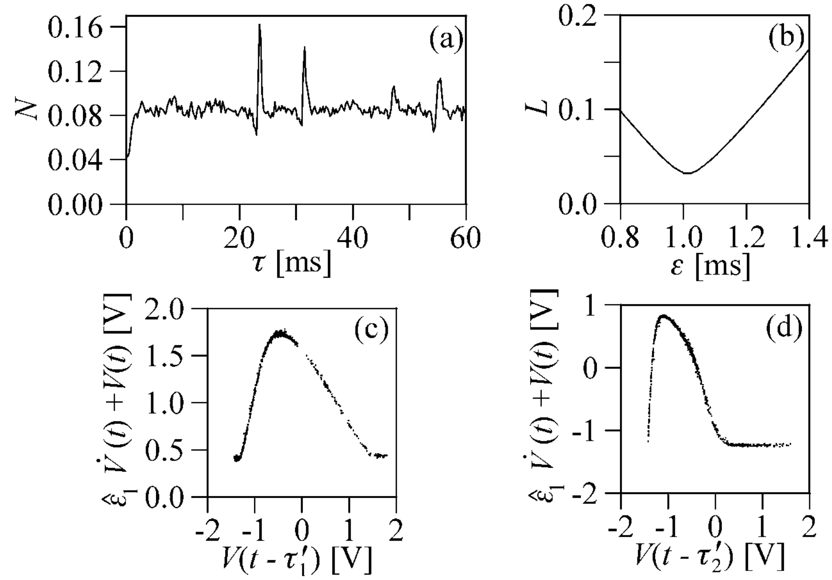

Figure 17. (a) Number N of pairs of extrema in the time series of the experimental system with two delays separated in time by τ. $N(\tau)$ is normalized to the total number of extrema in the time series. (b) Length L of a line connecting points ordered with respect to abscissa in the $V(t-\tau_1')=-1.1$ V section, as a function of ε. $L(\varepsilon)$ is normalized to the number of points in the section. $L_{\min}(\varepsilon)=L(1.01\ \text{ms})$. (c) Nonlinear function f_1 recovered up to the constant $c_1=f_2(V(t-\tau_2'))$, where $V(t-\tau_2')=-0.8$ V. (d) Nonlinear function f_2 recovered up to the constant $c_2=f_1(V(t-\tau_1'))$, where $V(t-\tau_1')=-1.1$ V.

8 Reconstruction of Coupled Time-Delay Systems

Let us consider the time-delayed feedback systems X_1 and X_2 described in the absence of coupling by the first-order delay-differential equation with single delay time

$$\varepsilon_{1,2}\dot{x}_{1,2}(t)=-x_{1,2}(t)+f_{1,2}(x_{1,2}(t-\tau_{1,2})), \tag{27}$$

where the indexes 1 and 2 correspond to the first and the second system, respectively. The systems X_1 and X_2 can be coupled in different ways. For instance, the system X_1 variable $x_1(t)$ multiplied by a coupling coefficient k_1 can be injected into the ring system X_2 at one of the three points indicated in Fig. 18 by the Arabic numerals 1–3. Similarly, the system X_2 variable $x_2(t)$ multiplied by a coupling coefficient k_2 can be injected into the ring system X_1 at different points indicated in Fig. 18 by the Roman numerals I–III. If the type of action of X_1 on X_2 is the same as the type of action of X_2 on X_1, then the dynamics of both coupled systems is described by one of the following equations

$$\varepsilon_{1,2}\dot{x}_{1,2}(t)=-x_{1,2}(t)+f_{1,2}(x_{1,2}(t-\tau_{1,2})+k_{2,1}x_{2,1}(t-\tau_{1,2})), \tag{28}$$

$$\varepsilon_{1,2}\dot{x}_{1,2}(t)=-x_{1,2}(t)+f_{1,2}(x_{1,2}(t-\tau_{1,2})+k_{2,1}x_{2,1}(t)), \tag{29}$$

$$\varepsilon_{1,2}\dot{x}_{1,2}(t)=-x_{1,2}(t)+f_{1,2}(x_{1,2}(t-\tau_{1,2}))+k_{2,1}x_{2,1}(t). \tag{30}$$

Equation (28) governs the both systems X_1 and X_2 for the type of coupling at which the first time-delay system acts on the second one at the point 1 and the second system acts upon the first one at the point I. We denote this type of coupling as 1/I. Equations (29) and (30) describe the both coupled systems for the types of coupling 2/II and 3/III, respectively. A block diagram of the coupled time-delay systems for the coupling type 3/III is shown in Fig. 19. If the systems X_1 and X_2 affect on each other in different ways, then they are described by different equations. For example, in the case of 1/II type of coupling, the system X_1 is given by Eq. (29) and the system X_2 is given by Eq. (28). Certainly, the variety of possible types of coupling between time-delay systems is very large. In this chapter we restrict our consideration to only three chosen types of linear coupling between two time-delay systems.

At first we recover the model equation of the system X_1, i.e., we estimate the parameters τ_1, ε_1, and k_2 and reconstruct the nonlinear function f_1. To determine the delay time τ_1 from the temporal realization $x_1(t)$ we exploit the considered above method based on the statistical analysis of time intervals between extrema in the time series. We find that this method of the delay time estimation can be successfully applied in the case where the system X_1 is affected by the system X_2 under the condition that this action is not followed by the appearance of a great number of additional extrema in the time series of X_1.

To recover the parameter ε_1, the nonlinear function f_1, and the coupling coefficient k_2 we propose a method using time series of both variables $x_1(t)$ and $x_2(t)$. At first, let us assume that the type of action of X_2 on X_1 is known a priori, i.e., we know the form of equation governing the dynamics of the time-delay system X_1. As an example, we consider the case described by Eq. (28), when the system X_2 variable is injected into the time-delayed feedback system X_1 before the element providing the delay (point I in Fig. 18). Let us write Eq. (28) for the system X_1 as

$$\varepsilon_1 \dot{x}_1(t) + x_1(t) = f_1(x_1(t-\tau_1) + k_2 x_2(t-\tau_1)) . \tag{31}$$

According to Eq. (31) it is possible to recover the function f_1 by plotting in a plane a set of points with coordinates $\left(x_1(t-\tau_1) + k_2 x_2(t-\tau_1), \varepsilon_1 \dot{x}_1(t) + x_1(t)\right)$. Since the parameters ε_1 and k_2 are unknown, one needs to plot $\varepsilon \dot{x}_1(t) + x_1(t)$ versus $x_1(t-\tau_1) + k x_2(t-\tau_1)$ under variation of ε and k, searching for a single-valued dependence in the plane $\left(x_1(t-\tau_1) + k x_2(t-\tau_1), \varepsilon \dot{x}_1(t) + x_1(t)\right)$, which is possible only for $\varepsilon = \varepsilon_1$ and $k = k_2$. As a quantitative criterion of single-valuedness in searching for ε_1 and k_2 we use the minimal length of a line $L(\varepsilon, k)$, connecting all points ordered with respect to the abscissa in the mentioned plane. The minimum $L_{\min}(\varepsilon, k)$ is observed at $\varepsilon = \varepsilon_1$ and $k = k_2$. The dependence of $\varepsilon_1 \dot{x}_1(t) + x_1(t)$ on $x_1(t-\tau_1) + k_2 x_2(t-\tau_1)$ for the defined ε_1 and k_2 reproduces the nonlinear function that can be approximated if necessary. The proposed technique uses all points of the time series. It allows one to estimate the parameters ε_1 and k_2 and to reconstruct the nonlinear function from short time series.

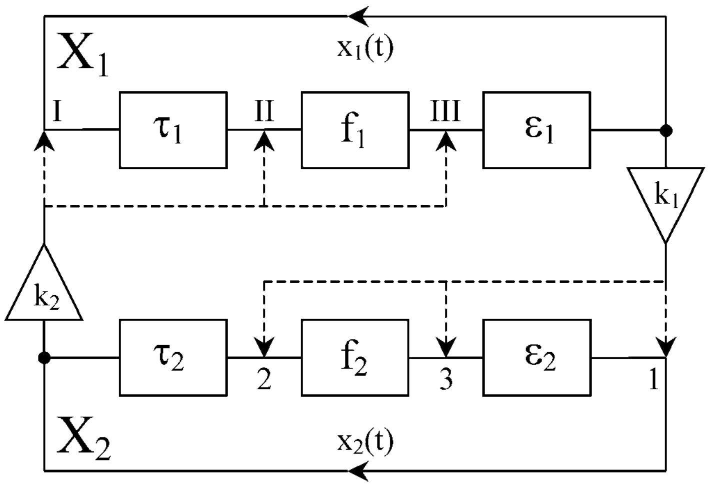

Figure 18. Block diagram of two coupled time-delay systems X_1 and X_2. The elements denoted as τ_1 and τ_2 provide a delay and the elements denoted as f_1 and f_2, and ε_1 and ε_2 provide the nonlinear and inertial transformations of oscillations, respectively. The elements k_1 and k_2 determine the strength of coupling between X_1 and X_2. Arabic numerals 1–3 designate points where the system X_1 acts on the system X_2. Roman numerals I–III designate points where X_2 acts on X_1.

Similarly it is possible to recover the nonlinear function f_1 and the parameters ε_1 and k_2 for the system X_1 described by Eq. (29) or Eq. (30) by plotting $\varepsilon\dot{x}_1(t)+x_1(t)$ versus $x_1(t-\tau_1)+kx_2(t)$ or $\varepsilon\dot{x}_1(t)+x_1(t)-kx_2(t)$ versus $x_1(t-\tau_1)$, respectively, under variation of ε and k. If we know that time-delay systems (27) are linearly coupled in one of the three considered ways, but we do not know at which point (I, II, or III) X_2 acts on X_1, we have to reconstruct each of the model equations (28)–(30) of the system X_1 and to define $L_{\min}(\varepsilon,k)$ for each of these equations. The single-valuedness of the recovered nonlinear function can be achieved only in the case of the true choice of the model equation. Hence, the smallest $L_{\min}(\varepsilon,k)$ from the three obtained ones will correspond to the true model choice. Thus, along with estimation of the parameters of coupled time-delay systems the method allows one to identify the type of coupling.

The time-delay system X_2 can be reconstructed from the time series of $x_2(t)$ and $x_1(t)$ in a similar way. The method allows us to estimate the parameters τ_2 and ε_2, to recover the nonlinear function f_2, and to define the coupling coefficient k_1 and the type of action of X_1 on X_2. Identifying the type of coupling between the systems and estimating the values of both coupling coefficients k_1 and k_2 we can judge of the character of interaction between the time-delay systems X_1 and X_2.

First we apply the method to the time series produced by two coupled identical time-delay systems described in the absence of coupling by the Mackey-Glass equation

$$\dot{x}_{1,2}(t) = -b_{1,2}x_{1,2}(t) + \frac{a_{1,2}x_{1,2}(t-\tau_{1,2})}{1+x_{1,2}^{c_{1,2}}(t-\tau_{1,2})}. \tag{32}$$

The types of action of the systems X_1 and X_2 on each other are chosen to be the same (Fig. 19). We use the 3/III type of coupling according to our classification. In this case the dynamics of both coupled systems is governed by Eq. (30). The system parameters are chosen to be $\tau_{1,2} = 300$, $a_{1,2} = 0.2$, $b_{1,2} = 0.1$, $c_{1,2} = 10$, $k_1 = 0.05$, and $k_2 = 0.1$ to produce a dynamics on a high-dimensional chaotic attractor. Part of the time series of the system X_1 is shown in Fig. 20(a). The time series is sampled in such a way that 300 points in time series cover a period of time equal to the delay time $\tau_1 = 300$. The data set consists of 10000 points and exhibits about 600 extrema as well as the time series of the system X_2.

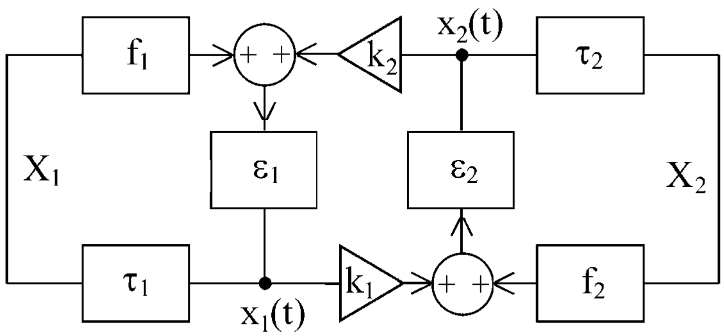

Figure 19. Block diagram of coupled time-delay systems for the 3/III type of coupling.

For various τ values we count the number *N* of situations when $\dot{x}_1(t)$ and $\dot{x}_1(t-\tau)$ are simultaneously equal to zero, normalize *N* to the total number of extrema in the time series, and construct the $N(\tau)$ plot [Fig. 20(b)]. The step of τ variation in Fig. 20(b) is equal to unity. The pronounced minimum of $N(\tau)$ takes place exactly at $\tau = \tau_1 = 300$.

The $L(\varepsilon, k)$ plot [Fig. 20(c)] allows us to recover the parameters ε_1 and k_2. To reduce the computation time we choose a large initial step of ε and *k* variation and then reduce it in the neighborhood of minimum $L(\varepsilon, k)$. In Fig. 20(c) the step of ε variation is set by 0.1 and the step of *k* variation is set by 0.01. The minimum of $L(\varepsilon, k)$ is observed at $\varepsilon = 10.1$ and $k = 0.10$. These values agree well with the true parameter values $\varepsilon_1 = 1/b_1 = 10$ and $k_2 = 0.1$. In Fig. 20(d) the recovered nonlinear function f_1 is shown. It coincides practically with the true nonlinear function. Note that for the construction of the $L(\varepsilon, k)$ plot and for the recovery of the function f_1 we use only 2000 points of the time series of $x_1(t)$ and $x_2(t)$.

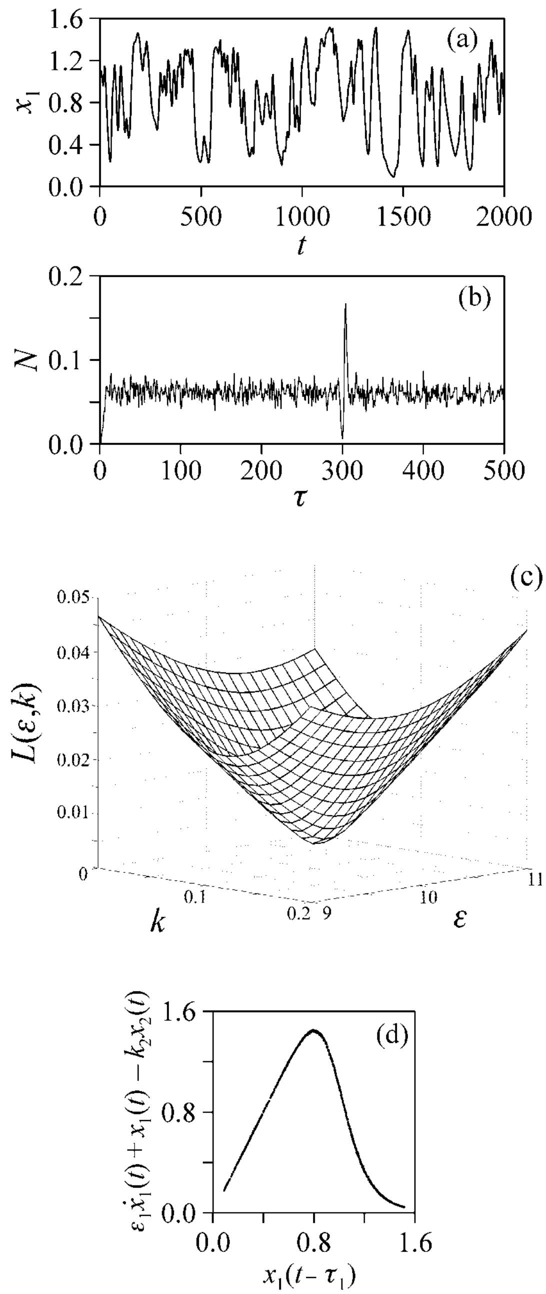

Figure 20. Reconstruction of the Mackey-Glass system X_1 coupled with the identical Mackey-Glass system X_2 for the 3/III type of coupling. (a) The time series of the system X_1. (b) Number N of pairs of extrema in the time series of X_1 separated in time by τ, as a function of τ. $N(\tau)$ is normalized to the total number of extrema in the time series. (c) The $L(\varepsilon, k)$ plot for the choice of the model equation in the form of Eq. (30). $L(\varepsilon, k)$ is normalized to the number of points. $L_{\min}(\varepsilon, k) = L(10.1, 0.10)$. (d) The recovered nonlinear function at $\tau_1 = 300$, $\varepsilon_1 = 10.1$, and $k_2 = 0.1$.

In a similar way we reconstruct the time-delay system X_2 and obtain the following estimation of its parameters: $\tau_2 = 300$, $\varepsilon_2 = 10.1$, and $k_1 = 0.05$. For the indicated above parameter values of two coupled identical systems (32) the method provides the detection of coupling presence and high accuracy of coupling coefficients estimation at $0.003 \le k_{1,2} \le 0.3$. It should be noted that the method is still efficient for sufficiently high levels of noise. For example, we apply the method to the data produced by adding a zero-mean Gaussian white noise to the time series of both coupled identical Mackey-Glass equations. For the case where the additive noise has a standard deviation of up to 20% of the standard deviation of the data without noise, we obtain the same values of the recovered parameters as in the considered above case of noise absence. However, the quality of the nonlinear function recovery deteriorates with the noise increasing.

Let us consider a more general case of coupled nonidentical noisy time-delay systems X_1 and X_2 with different types of action on each other. We apply the method to the time series of two coupled Mackey-Glass equations for the 1/II type of coupling at $\tau_1 = 300$, $\tau_2 = 400$, $a_1 = 0.2$, $a_2 = 0.3$, $b_{1,2} = 0.1$, $c_{1,2} = 10$, $k_1 = 0.05$, and $k_2 = 0.1$. To investigate the robustness of the method to perturbations we analyze the time series of X_1 and X_2 both corrupted by additive Gaussian white noise. Figure 21 illustrates the obtained results for a noise level of 10%.

The presence of noise in time series brings into existence spurious extrema. These extrema are not caused by the intrinsic dynamics of a system and temporal distances between them are random. To smooth the time series corrupted by noise and to reduce the number of extrema caused by noise we use more nearest-neighbor points in the procedure of local approximation while estimating derivatives from data in comparison with the case of noise absence. In spite of the noise presence the pronounced minimum of the $N(\tau)$ plot constructed for the system X_1 time series is observed at $\tau = \tau_1 = 300$ [Fig. 21(a)] and the pronounced minimum of $N(\tau)$ for the time series of X_2 is observed at $\tau = \tau_2 = 400$ [Fig. 21(b)]. The $L(\varepsilon, k)$ plot, constructed for the system X_1 recovery in the form of Eq. (29), demonstrates the minimum at $\varepsilon = 10.0$ and $k = 0.10$ giving the accurate estimation of ε_1 and k_2. The location of the absolute minimum of the $L(\varepsilon, k)$ plot, constructed for the system X_2 recovery in the form of Eq. (28), allows us to obtain the following estimation of the parameters: $\varepsilon_2 = 10.1$ and $k_1 = 0.05$. The recovered nonlinear functions f_1 and f_2 are presented in Figs. 21(c) and (d), respectively.

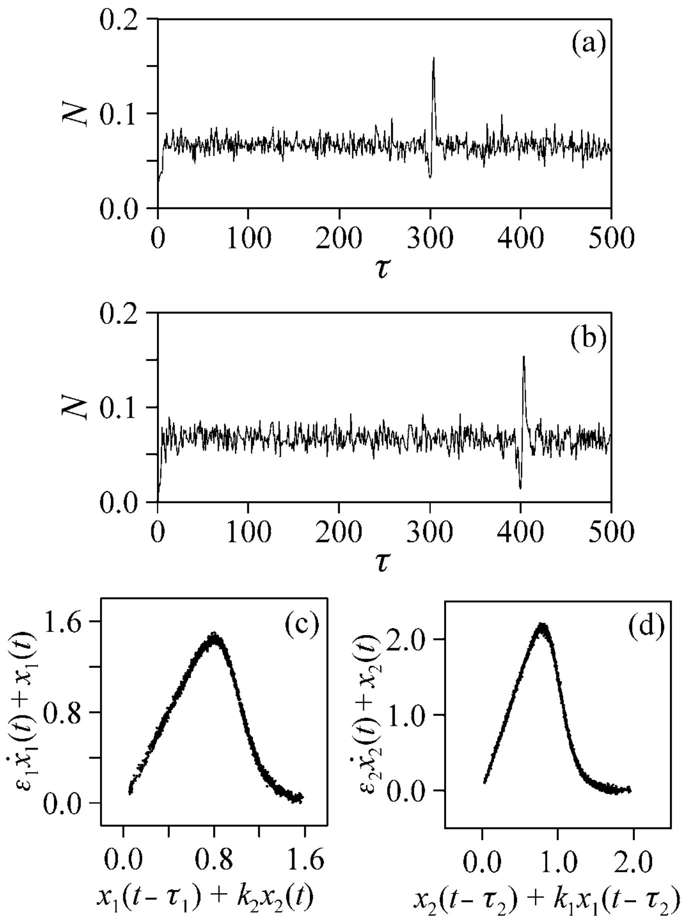

Figure 21. Reconstruction of coupled nonidentical Mackey-Glass systems from data corrupted by additive Gaussian white noise for noise level of 10% and 1/II type of coupling. (a) Number N of pairs of extrema in the system X_1 time series separated in time by τ normalized to the total number of extrema. (b) Number N of pairs of extrema in the system X_2 time series separated in time by τ normalized to the total number of extrema. (c) The recovered nonlinear function f_1 at $\tau_1 = 300$, $\varepsilon_1 = 10.0$, and $k_2 = 0.10$. (d) The recovered nonlinear function f_2 at $\tau_2 = 400$, $\varepsilon_2 = 10.1$, and $k_1 = 0.05$.

The next example is the method application to experimental time series gained from two coupled electronic oscillators with delayed feedback. A block diagram of the experimental setup is shown in Fig. 22. The delay of the signal $V_1(t)$ for time τ_1 and the delay of the signal $V_2(t)$ for time τ_2 are provided by the delay lines DL-1 and DL-2, respectively, constructed using digital elements or computer. The delay lines are practically dispersion free while the signal band defined by the filter parameters lies within the band of analog-to-digital converters. The conversion frequencies of analog-to-digital converters are about 100 kHz and the cutoff frequencies of the filters are about 1 kHz and 2 kHz. The role of nonlinear devices ND-1 and ND-2 is played in the oscillators by the amplifiers with the transfer functions f_1 and f_2, respectively. These nonlinear devices ND-1 and ND-2 were constructed using bipolar transistors and field-effect transistors, respectively. The inertial properties of oscillators are defined by low-frequency first-order *RC* filters R_1C_1 and R_2C_2, which parameters specify ε_1 and ε_2. The coupling of oscillators is realized using summing amplifiers with gains k_1 and k_2. The type of coupling corresponds to the case 1/III according to our classification.

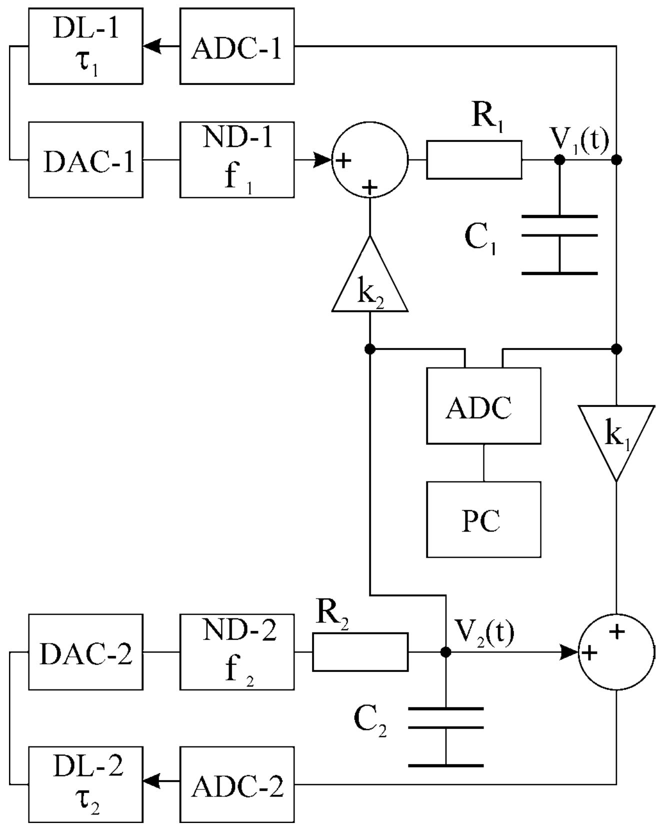

Figure 22. Block diagram of the experimental system of coupled electronic oscillators with delayed feedback for the 1/III type of coupling. DL-1 and DL-2 are the delay lines, ND-1 and ND-2 are the nonlinear devices, ADC-1 and ADC-2 are the analog-to-digital converters, and DAC-1 and DAC-2 are the digital-to-analog converters of the first and the second oscillator, respectively. ADC is a two-channel analog-to-digital converter and PC is a computer.

In the absence of coupling the considered oscillators are given by

$$R_{1,2}C_{1,2}\dot{V}_{1,2}(t) = -V_{1,2}(t) + f_{1,2}(V_{1,2}(t-\tau_{1,2})), \tag{33}$$

where $V_{1,2}(t)$ and $V_{1,2}(t-\tau_{1,2})$ are the delay line input and output voltages, respectively, $R_{1,2}$ and $C_{1,2}$ are the resistances and capacitances of the filter elements in the first and the second oscillator, respectively. Equation (33) is of the form (27) with $\varepsilon_{1,2} = R_{1,2}C_{1,2}$.

We record the signals $V_1(t)$ and $V_2(t)$ using a two-channel analog-to-digital converter ADC (Fig. 22) with the sampling frequency $f_s = 10$ kHz at $\tau_1 = 23$ ms, $\tau_2 = 31.7$ ms, $R_1C_1 = 0.48$ ms, $R_2C_2 = 1.01$ ms, $k_1 = -0.1$, and $k_2 = 0.1$. The parts of the time series of the signals $V_1(t)$ and $V_2(t)$ are presented in Figs. 23(a) and (b), respectively. For the step of τ variation equal to the sampling time $T_s = 0.1$ ms, the pronounced minimum of $N(\tau)$ takes place at $\tau = 23.0$ ms [Fig. 23(c)] for the first oscillator and at $\tau = 31.7$ ms [Fig. 23(d)] for the second oscillator.

To construct the $L(\varepsilon, k)$ plot we use the step of ε variation equal to 0.01 ms and the step of k variation equal to 0.01. Reconstructing the model of the oscillator X_1 in the form of Eq. (30) we obtain the minimum of $L(\varepsilon, k)$ at $\varepsilon = 0.46$ ms and $k = 0.10$ that are close to the true values of ε_1 and k_2. The recovered nonlinear function [Fig. 24(a)] coincides closely with the true transfer function f_1 of the nonlinear element of the first oscillator.

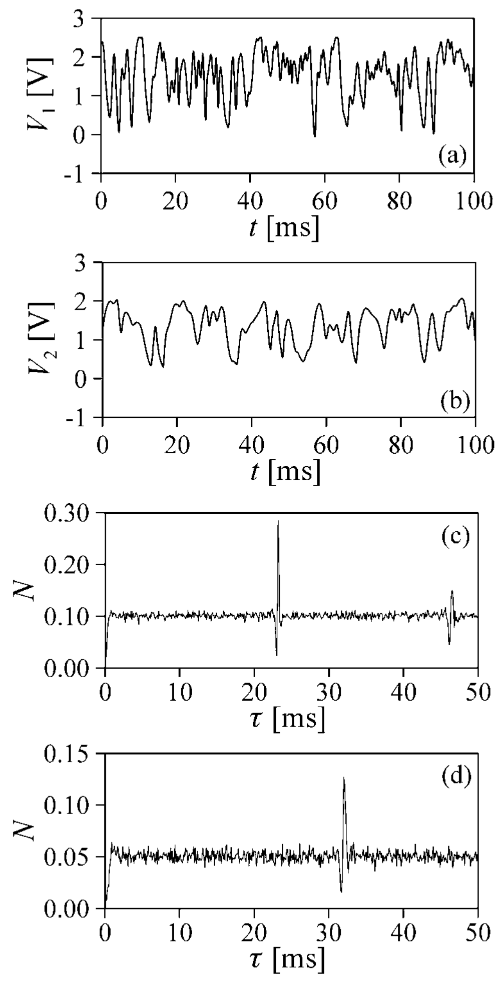

Figure 23. Experimental time series of the first (a) and the second (b) coupled electronic oscillators with delayed feedback. Number N of pairs of extrema in the time series of the oscillator X_1 (c) and the oscillator X_2 (d), separated in time by τ, as a function of τ. $N(\tau)$ is normalized to the total number of extrema in the time series.

Reconstructing the system X_2 in the form of Eq. (28) we observe the minimum of $L(\varepsilon, k)$ at $\varepsilon = 1.06$ ms and $k = -0.10$ that give a close estimation of ε_2 and k_1. In Fig. 24(b) the recovered nonlinear function of the system X_2 is shown. This function coincides closely with the true transfer function f_2 of the nonlinear element of the second oscillator. If it is known that the system X_2 is governed by one of the three model equations (28)–(30) but it is not known exactly which of the three types of linear coupling takes place, then one has to recover each of the model equations (28)–(30) for the system X_2 and to define $L_{\min}(\varepsilon, k)$ for each of the three cases. For the choice of the system X_2 model in the form of Eq. (29) we obtain $L_{\min}(\varepsilon, k) = L(0.98 \text{ ms}, 0.00) = 0.135$. Reconstructing the model equation of the system X_2 in the form of Eq. (30) we obtain $L_{\min}(\varepsilon, k) = L(0.97 \text{ ms}, 0.01) = 0.134$. In both cases $L_{\min}(\varepsilon, k)$ is normalized to the number of points. The results of the nonlinear function f_2 recovery for the choice of the model equation in the form of Eqs. (29) and (30) are shown in Figs. 24(c) and (d), respectively. From the three plots presented in Figs. 24(b)–(d) only the plot in Fig. 24(b) demonstrates a set of points that is close to a single-valued curve. In this case $L_{\min}(\varepsilon, k) = L(1.06 \text{ ms}, -0.10) = 0.035$ that is significantly less than in the two other cases. This result indicates that the model equation of the second oscillator has the form of Eq. (28).

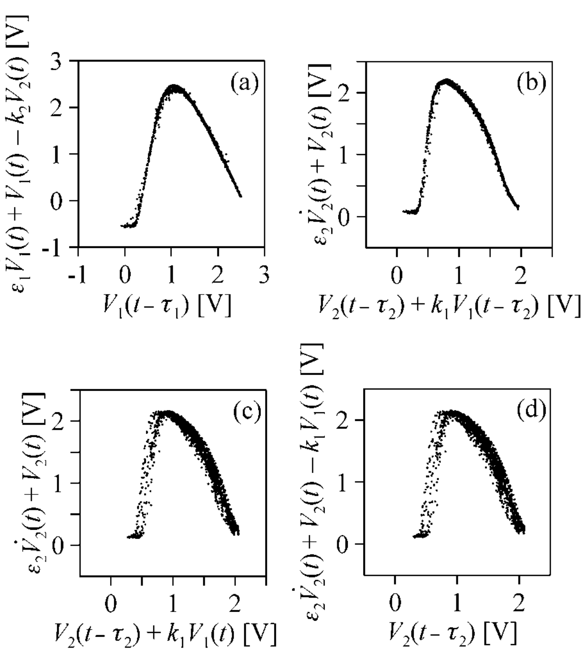

Figure 24. Reconstruction of nonlinear functions of coupled electronic oscillators with delayed feedback. (a) The recovered nonlinear function f_1 at $\tau_1 = 23.0$ ms, $\varepsilon_1 = 0.46$ ms, and $k_2 = 0.10$. (b)–(d) Results of the nonlinear function f_2 recovery for the choice of the second oscillator model equation in the form of Eqs. (28)–(30), respectively, at the recovered parameters $\varepsilon_2 = 1.06$ ms and $k_1 = -0.10$ (b), $\varepsilon_2 = 0.98$ ms and $k_1 = 0.00$ (c), and $\varepsilon_2 = 0.97$ ms and $k_1 = 0.01$ (d).

We use the smallest value of $L_{\min}(\varepsilon, k)$ from the three obtained ones as a criterion for the identification of the right coupling. But if the minimal value of $L_{\min}(\varepsilon, k)$ is close to the values of $L_{\min}(\varepsilon, k)$ for the other two projections, it cannot be considered as the reliable criterion for identification of the coupling type. To ensure the validity of this criterion we use it only if the minimal value of $L_{\min}(\varepsilon, k)$ is less than the other values of $L_{\min}(\varepsilon, k)$ by a factor of two or a greater factor. The difference between the values of $L_{\min}(\varepsilon, k)$ for different projections depends not only on the level of noise but also on the coupling coefficient. For small coupling values it is difficult to identify the a priori unknown type of coupling. For example, for the considered above parameter values of coupled Mackey-Class equations and the coupling coefficient $k_2 = 0.1$ we were able to identify with certainty the type of action of the system X_2 on the system X_1 for additive noise levels up to 20%.

The proposed method can be also used for the reconstruction of a time-delay system affected by a system that is not a time-delay system and for the estimation of strength of this driving. In contrast to the other methods of detection of coupling between the systems from time series [37–39] the proposed technique is able to define not only the direction but also the value of coupling.

The procedure of the coupling coefficients estimation considered with coupled time-delay systems like (28)–(30) for the three chosen types of linear coupling can be successfully applied to many other types of coupling between scalar time-delay systems of the form (27). For example, in the case of diffusive coupling between time-delay systems X_1 and X_2 described by the equation

$$\varepsilon_{1,2}\dot{x}_{1,2}(t) = -x_{1,2}(t) + f_{1,2}(x_{1,2}(t-\tau_{1,2})) + k_{2,1}(x_{2,1}(t) - x_{1,2}(t)), \tag{34}$$

it is possible to recover the nonlinear functions $f_{1,2}$ and the parameters $\varepsilon_{1,2}$ and $k_{2,1}$ of the systems $X_{1,2}$ by plotting $\varepsilon_{1,2}\dot{x}_{1,2}(t) + x_{1,2}(t) - k_{2,1}(x_{2,1}(t) - x_{1,2}(t))$ versus $x_{1,2}(t-\tau_{1,2})$ under variation of ε and k. The method is also efficient for some types of nonlinear coupling between the systems X_1 and X_2 if the coupling term does not contain the unknown functions g_1 or g_2. In the case of the coupling term $k_{2,1}(g_{2,1}(x_{2,1}(t)) - g_{1,2}(x_{1,2}(t)))$ and other similar terms the method cannot be used. It should be noted that in the general case for the reconstruction of coupled time-delay systems and their coupling coefficients estimation we must know the type of coupling defining the embedding spaces to which the trajectories of time-delay systems are projected.

In principle, it is possible to extend the proposed method to time-delay systems described in the absence of coupling by delay-differential equation of higher order than Eq. (27). However, the higher the order of equation, the more parameters of coupled systems have to be recovered. As the result, the time of computation significantly increases and the quality of reconstruction deteriorates since the procedure involves numerical calculation of the higher order derivatives. Similar problems arise in the case of three and more coupled time-delay systems.

9 Application to Chaotic Communication

The discovery of the phenomenon of synchronization in chaotic systems [40] has given rise to active development of secure communication methods using chaotic signal as a carrier [41–

44]. Chaotic communication systems are particularly attractive due to the broadband power spectrum of chaotic signals, high rates of information transmission, and tolerance to sufficiently high levels of noise. Besides, many chaotic communication schemes are simply realized and demonstrate a rich variety of different oscillating regimes. However, many chaotic communication schemes are not as secure as expected and can be successfully unmasked [45–49]. To improve the security of data transmission it has been proposed to employ time-delay systems demonstrating chaotic dynamics of a very high dimension [26–31]. However, even in communication schemes using masking chaotic signals of time-delay systems the hidden message can be extracted in certain cases by an eavesdropper [11, 12]. In this chapter we consider different ways for encryption and decryption of information in communication schemes based on time-delay systems and propose a technique for extracting a hidden message in the case when the transmitter parameters are unknown.

A block diagram of a transmitter, representing the ring system composed of delay, nonlinear, and inertial elements, is shown in Fig. 2. For the case when the filter is a low-frequency first-order filter, this transmitter is described in the absence of information signal by the delay-differential equation (2). The information signal $m(t)$ can be injected into the ring system (2) at different points denoted in Fig. 2 by the numerals 1, 2, and 3. Depending on the point at which the message signal is injected into the feedback circuit of the transmitter, the system's dynamics is governed by one of the following equations:

$$\varepsilon_1 \dot{x}(t) = -x(t) + f(x(t-\tau_1) + m(t-\tau_1)), \tag{35}$$

$$\varepsilon_1 \dot{x}(t) = -x(t) + f(x(t-\tau_1) + m(t)), \tag{36}$$

$$\varepsilon_1 \dot{x}(t) = -x(t) + f(x(t-\tau_1)) + m(t). \tag{37}$$

Equation (35) corresponds to the case when the signal $m(t)$ is injected into the transmitter at the point 1. The cases of information signal injection at the points 2 and 3 are described by Eqs. (36) and (37), respectively. With this nonlinear mixing the information signal is directly involved in the formation of a complicated dynamics of the chaotic system. The signal $s(t)$ transmitted into the communication channel can be also taken from different points of the ring system indicated in Fig. 2 by the numerals 1–3. Thus, there are nine different ways for realizing the transmitter depicted in Fig. 2.

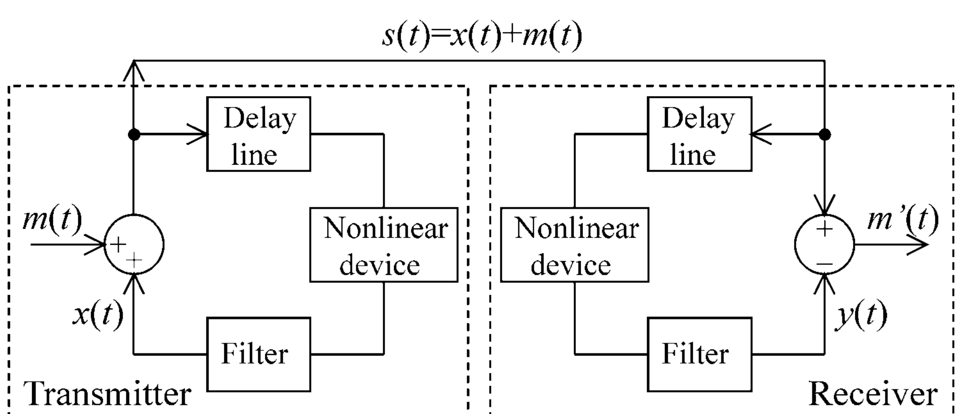

Figure 25. Block diagram of the chaotic communication system for the case 1/1.

Similar approach for the information encryption in delayed nonlinear feedback systems has been considered in Ref. [31]. The possibility of the message signal recovery at the receiver was discussed in Ref. [31] for different ways of the information signal injection into the time-delay system and different output points of the transmitter. The configuration and the parameters of the transmitter were assumed to be known to the authorized receiver. Nevertheless, in a number of cases the message recovery required processing of the signal at the receiver output, including determination of the reciprocal function of the nonlinear element. Since the transfer function of a nonlinear element is not necessarily one-to-one, this transformation may be incorrect. In such cases, we suggest using an approximate approach for recovering the information signal. This approach allows one to avoid inverse transformation. Moreover, using our method the information signal can be extracted from the transmitted signal $s(t)$ even in the case when the transmitter parameters are a priori unknown.

Let us consider different configurations of the transmitter shown in Fig. 2 and determine the corresponding signals at the output of the receiver being an identical copy of the transmitter. Figure 25 illustrates the communication scheme based on the transmitter configuration denoted as 1/1. In this case, with the help of a summator the information signal $m(t)$ is added at the point 1 to the chaotic signal $x(t)$ of the transmitter whose dynamics is described by Eq. (35), and the signal $s(t) = x(t) + m(t)$ is transmitted into the communication channel also from the point 1.

The receiver is composed of the same elements as the transmitter, except the summator replaced by a subtracter breaking the feedback circuit. The receiver equation is

$$\varepsilon_1 \dot{y}(t) = -y(t) + f(x(t-\tau_1) + m(t-\tau_1)) . \tag{38}$$

At the output of the subtracter we have the extracted information signal $m'(t) = x(t) + m(t) - y(t)$.

If the transmitter and the receiver are composed of identical elements, they become completely synchronized after the transient process. The difference between the oscillations of systems (35) and (38), $\Delta(t) = x(t) - y(t)$, decreases in time for any $\varepsilon_1 > 0$, since $\dot{\Delta}(t) = -\dfrac{\Delta}{\varepsilon_1}$. As the result of synchronization, $x(t) = y(t)$ and $m'(t) = m(t)$.

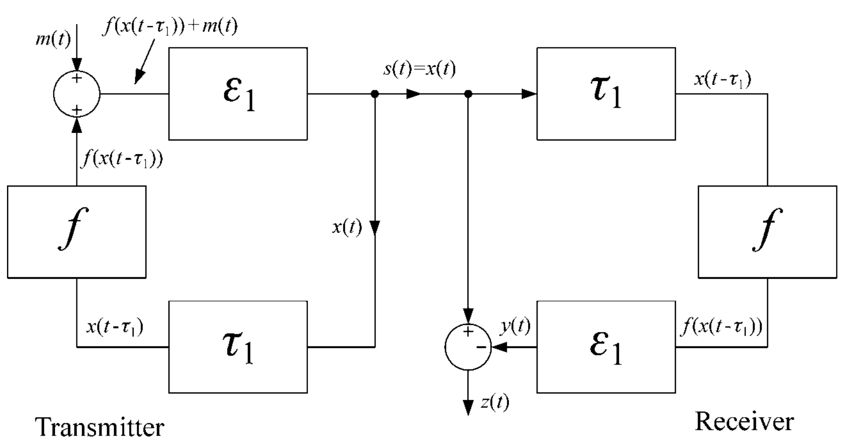

Figure 26. Block diagram of the chaotic communication system for the case 3/1.

If we take away the delay line in the receiver, Eq. (38) will take the form

$$\varepsilon_1 \dot{y}(t) = -y(t) + f(x(t) + m(t)) . \tag{39}$$

In this case the receiver synchronizes with the transmitter in such a way, that $x(t) = y(t - \tau_1)$ or, equivalently, $x(t + \tau_1) = y(t)$. In other words, at time t the receiver (39) synchronizes with the future state of the transmitter (35) at time $t + \tau_1$. It is the case of anticipating synchronization [50]. The delay line will be necessary to extract the information signal. If we delay the signal $y(t)$ by τ_1 and feed the signal $y(t - \tau_1)$ at the subtracter input, then we receive $m'(t) = x(t) + m(t) - y(t - \tau_1) = m(t)$ at the subtracter output.

Figure 26 shows the communication scheme based on the transmitter configuration 3/1. In this case, the information signal $m(t)$ is added at the point 3 (see Fig. 2) to the chaotic signal of the transmitter whose dynamics is described by Eq. (37), and the signal $s(t) = x(t)$ is transmitted into the communication channel from the point 1. The receiver equation is

$$\varepsilon_1 \dot{y}(t) = -y(t) + f(x(t - \tau_1)) . \tag{40}$$

At the output of the subtracter we have the signal $z(t) = x(t) - y(t)$.

Table I. The difference signal $z(t)$ at the output of the receiver for different points of information signal injection into the feedback circuit of the transmitter and different points of the signal output.

Input point	Output point		
	1	2	3
1	$m(t)$	$m(t-\tau_1)$	$f[x(t-\tau_1)+m(t-\tau_1)]-$ $f[x(t-\tau_1)]$
2	$\varepsilon_1[\dot{y}(t)-\dot{x}(t)]+$ $f[x(t-\tau_1)+m(t)]-$ $f[x(t-\tau_1)]$	$m(t)$	$f[x(t-\tau_1)+m(t)]-$ $f[x(t-\tau_1)]$
3	$x(t)-y(t)$	$x(t-\tau_1)-y(t-\tau_1)$	$m(t)$

The values of the signal $z(t)$ at the receiver output are presented in Table I for various configurations of the communication scheme. In the simplest cases 1/1, 2/2, and 3/3, where the information signal is injected into the feedback circuit of the transmitter and simultaneously transmitted into the communication channel, we immediately have the extracted message signal $z(t) = m(t)$ at the output of the receiver. In these cases the quality of extraction of the message $m(t)$ does not depend on its amplitude and frequency characteristics. By this is meant that for the considered configurations the communication schemes allow one to transmit complicated information signals without distortion. For the case 1/2 the information signal is also recovered accurately, but with the delay τ_1.

For the other five configurations of the communication scheme the procedure of the message signal extraction is more complicated since the processing of the signal $z(t)$ at the receiver output is required. For example, for recovering the information signal in the case 3/1 depicted in Fig. 26, let us subtract Eq. (40) describing the dynamics of the receiver from Eq. (37) for the transmitter. The expression for $m(t)$ takes the form

$$m(t) = \varepsilon_1(\dot{x}(t) - \dot{y}(t)) - (x(t) - y(t)) . \tag{41}$$

Taking into account that $z(t) = x(t) - y(t)$, the information signal can be obtained from the signal at the receiver output as follows:

$$m(t) = \varepsilon_1 \dot{z}(t) - z(t) . \tag{42}$$

In a similar way one can recover the signal $m(t)$ for the case 3/2:

$$m(t) = \varepsilon_1 \dot{z}(t - \tau_1) - z(t - \tau_1) . \tag{43}$$

In the communication system 2/3 the difference signal at the output of the receiver is

$$z(t) = f(x(t - \tau_1) + m(t)) - f(x(t - \tau_1)) . \tag{44}$$

Assuming that the information signal $m(t)$ is small in comparison with $x(t)$, let us expand the first term in Eq. (44) in a Taylor series and restrict our consideration to the two first terms of the expansion:

$$f(x(t - \tau_1) + m(t)) \approx f(x(t - \tau_1)) + \frac{df(x(t - \tau_1))}{dx} m(t) . \tag{45}$$

This assumption is justified because the level of information signal in the communication schemes with nonlinear mixing must be sufficiently low, otherwise the chaotic signal may not provide enough masking [43]. From Eqs. (44) and (45) we obtain

$$m(t) \approx \frac{z(t)}{df(x(t - \tau_1))/dx} . \tag{46}$$

Equation (46) can be used also for approximate recovery of the message signal in the case 1/3. However, the recovered message signal is delayed by τ_1 in this case.

For the case 2/1 the message signal $m(t)$ can be approximately determined as follows:

$$m(t) \approx \frac{z(t) + \varepsilon_1 \dot{z}(t)}{df(x(t - \tau_1))/dx} . \tag{47}$$

The security of chaotic communication systems is based on the assumption that the parameters of the chaotic transmitter are known only to the authorized receiver having an identical copy of the transmitter. However, the information signal $m(t)$ masked by the considered communication schemes in such a way, that its presence is imperceptible in the communication channel, can be extracted by an unauthorized listener from the transmitted signal $s(t)$. Using the methods considered in Secs. III and IV it is possible to recover the parameters of the chaotic transmitter governed in the absence of message by delay-differential equation (2). These methods are still efficient in the presence of message in the transmitted signal if the message signal has small amplitude. In this case the information signal can be considered as noise deteriorating the accuracy of the transmitter parameters estimation. We have found out that our technique of time-delay system recovery provides sufficiently accurate estimation of the system parameters for noise levels up to 10%. To ensure the security of message transmission, the level of information signal in the considered communication systems is usually much lower [43]. Knowing the parameters of the transmitter one can construct the receiver and extract the message signal.

At first we consider the procedure of hidden message recovery without knowing the transmitter parameters for the simplest case 1/1. We apply the method to a time series produced by nonlinear mixing of the chaotic signal of the Mackey-Glass system (11) and the frequency-modulated harmonic signal

$$m(t) = A \sin(2\pi f_c t - B \cos(2\pi f_m t)) , \tag{48}$$

where A defines the message amplitude, f_c is the central frequency of the power spectrum of the signal, B is the frequency modulation index, and f_m is the modulation frequency. As a bandpass signal, the frequency-modulated harmonic signal better imitates the structure of speech and music signals than a simple harmonic signal. With a fourth-order Runge-Kutta method for delay-differential equations we record 50000 points with the sampling interval $h = 0.5$. Parts of the time series and the power spectra of frequency-modulated signal $m(t)$ and the transmitted chaotic signal $s(t) = x(t) + m(t)$ are presented in Figs. 27(a) and (b). As can be seen from these figures, the amplitude of the information signal comprises less than 1% of the amplitude of the chaotic carrier and the presence of message is not noticeable in the power spectrum of the transmitted signal $s(t)$.

Figures 27(c)–(d) illustrate the reconstruction of the transmitter parameters. To construct the $N(\tau)$ plot [Fig. 27(c)] we use 20000 points of the time series of $s(t)$. The time series exhibits about 600 extrema and $N(\tau)$ is normalized to their total number. The step of τ variation in Fig. 27(c) is equal to the integration step $h = 0.5$. The location of the absolute minimum of $N(\tau)$ allows one to estimate the delay time, $\tau_1' = 300.0$. Note that we obtain the same values of τ_1' for a time series whose length is shorter by a factor of 3.

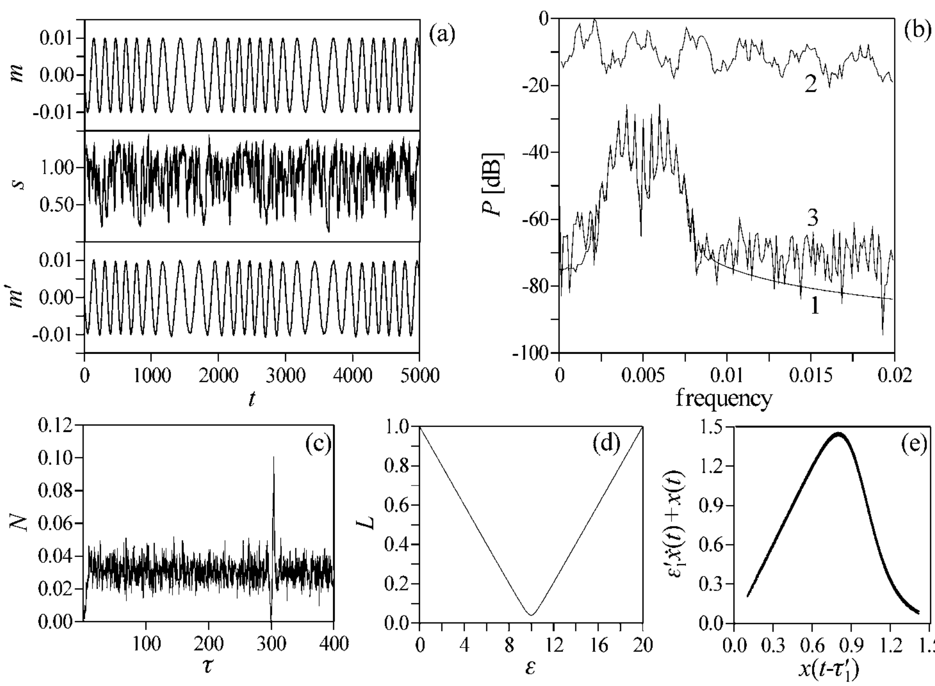

Figure 27. (a) The frequency-modulated harmonic signal $m(t)$ for $A = 0.01$, $B = 3$, $f_c = 5\times10^{-3}$, and $f_m = 5\times10^{-4}$, the transmitted signal $s(t)$ for $a = 0.2$, $b = 0.1$, $c = 10$, and $\tau_1 = 300$, and the extracted frequency-modulated harmonic signal $m'(t)$. (b) The power spectra of the signals (1) $m(t)$, (2) $s(t)$, and (3) $m'(t)$. (c) The $N(\tau)$ plot. $N_{\min}(\tau) = N(300.0)$. (d) The $L(\varepsilon)$ plot. $L_{\min}(\varepsilon) = L(10.0)$. (e) The recovered nonlinear function.

To construct the $L(\varepsilon)$ plot [Fig. 27(d)] we use only 2000 points of $s(t)$ realization. The step of ε variation is set by 0.1. The minimum of $L(\varepsilon)$ takes place at $\varepsilon_1' = 10.0$ ($\varepsilon_1 = 1/b = 10$). The nonlinear function recovered using the estimated τ_1' and ε_1' is shown in Fig. 27(e). For the approximation of the recovered function we use polynomials of different degree. The approximating function is sufficiently close to the nonlinear function of the Mackey-Glass equation and ensures a high quality of synchronous response of the receiver if the degree of the polynomial is greater than 11. To increase the accuracy of polynomial approximation we use all points of the time series at the reconstruction of the nonlinear function.

The more accurate is the estimation of the transmitter parameters, the higher is the quality of synchronous chaotic response of the receiver and, as a consequence, the higher is the quality of the message extraction. The quality of the recovery of the system parameters can be estimated by the level of the desynchronization noise (Fig. 28) leading to a worse quality of synchronous chaotic response. It follows from Fig. 28 that the level of the desynchronization noise is about 0.1% of the level of the chaotic signal and can achieve 10% of the amplitude of the information signal [Fig. 27(a)] at the receiver output. Part of the time series and the power spectrum of the extracted frequency-modulated signal $m'(t)$ are presented in Figs. 27(a) and (b), respectively.

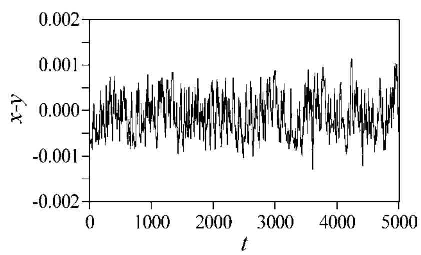

Figure 28. The noise of desynchronization of the transmitter (35) and the recovered receiver (38) in the absence of information signal.

As another example, we consider an experimental communication system of 1/1 type using the chaotic signal of an electronic oscillator with delayed feedback. For the case when the filter is a low-frequency first-order *RC*-filter this oscillator is given by Eq. (9). The chaotic signal $V(t)$ of the system (9) is nonlinearly mixed with the harmonic signal $m(t) = A\sin(2\pi f_c t)$ with amplitude A and frequency f_c. The transmitted signal is $s(t) = V(t) + m(t)$. We record the signals $m(t)$ and $s(t)$ using an analog-to-digital converter with the sampling frequency $f_s = 4$ kHz. In Figs. 29(a) and (b) parts of the time series and power spectra of these signals are presented.

Figures 29(c)–(d) illustrate the reconstruction of the transmitter. Since the delay time $\tau_1 = 54.7$ ms is not a multiple of the sampling time $T_s = 0.25$ ms, the recovery of τ_1 can not be absolutely accurate. For the step of τ variation equal to T_s the minimum of $N(\tau)$ takes place at $\tau_1' = 54.75$ ms [Fig. 29(c)]. The $L(\varepsilon)$ plot, constructed with τ_1' and the step of ε variation equal to 0.025 ms, demonstrates the minimum at $\varepsilon_1' = 4.2$ ms [Fig. 29(d)] ($\varepsilon_1 = 4.21$ ms). The recovered nonlinear function is shown in Fig. 29(e). The approximation of this function with a polynomial of degree two allows us to obtain a high-quality synchronous response of the receiver and, as the result, a sufficiently qualitative extraction of the hidden message. Part of the time series and the power spectrum of the extracted harmonic signal are shown in Figs. 29(a) and (b). Thus, the extraction of hidden information is possible in spite of the presence of noise inherent in a real system and the absence of multiplicity between the characteristic temporal scales of the chaotic transmitter and the sampling time, which result in the inaccurate estimation of the parameters.

Let us apply our method for extracting the hidden message in the more complicated cases of communication schemes 3/1 and 2/3. We consider the recovery of the frequency-modulated harmonic signal (48) nonlinearly mixed with the chaotic signal of the Mackey-Glass system (11). The parameters of the information signal and the Mackey-Glass system are chosen the same as in the considered above case 1/1. The temporal realizations of the transmitted signals $s(t)$ are qualitatively similar to the one shown in Fig. 27(a). For the configuration 3/1 of the transmitter (see Fig. 26) the procedure of its parameters recovery is the same as in the considered case 1/1. Part of the time series of the extracted frequency-modulated harmonic signal $m'(t)$ calculated using Eq. (42) is presented in Fig. 30(a). The power spectrum of this signal is shown in Fig. 30(b). The extracted message signal is sufficiently close to the true information signal $m(t)$ depicted in Fig. 27(a) and the power spectrum of $m'(t)$ is qualitatively similar to the power spectrum of $m(t)$ [Fig. 27(b)].

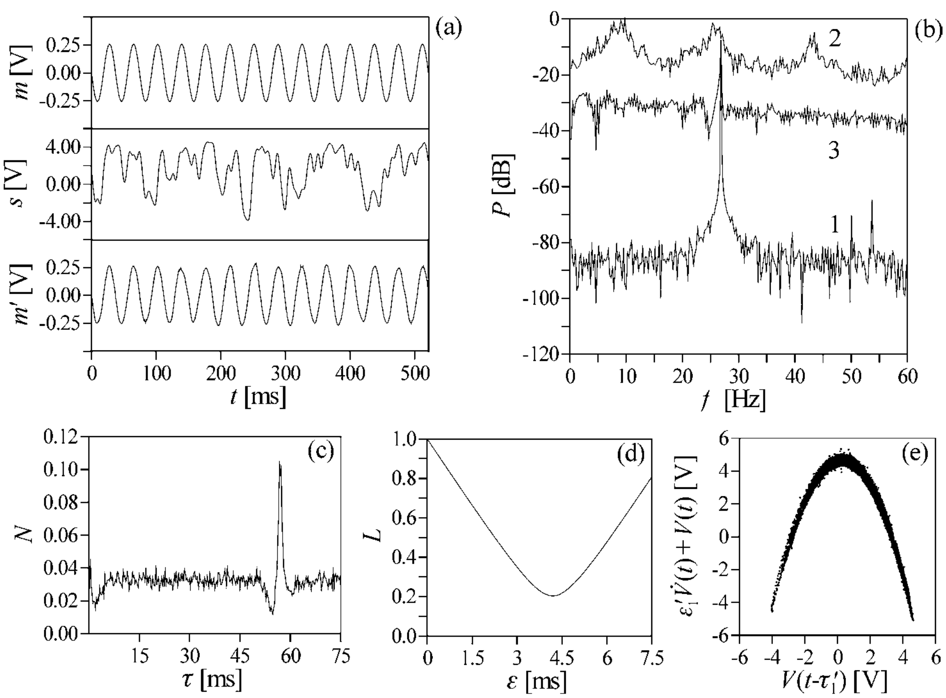

Figure 29. (a) The original message signal $m(t)$ with $A = 0.25$ V and $f_c = 27$ Hz, the transmitted signal $s(t)$ for $\tau_1 = 54.7$ ms and $RC = \varepsilon_1 = 4.21$ ms, and the extracted harmonic signal $m'(t)$. (b) The power spectra of the signals (1) $m(t)$, (2) $s(t)$, and (3) $m'(t)$. (c) The $N(\tau)$ plot. $N_{\min}(\tau) = N(54.75\ \text{ms})$. (d) The $L(\varepsilon)$ plot. $L_{\min}(\varepsilon) = L(4.2\ \text{ms})$. (e) The recovered nonlinear function.

For the transmitter configuration denoted as 2/3 the procedure of the parameters recovery is different from the considered one since the signal $s(t) = f[x(t-\tau_1) + m(t)]$ transmitted into the communication channel is taken from the points 3 of the ring system with nonlinear time-delayed feedback (Fig. 2).

For various τ values we count the number N of situations when $\dot{s}(t)$ and $\dot{s}(t-\tau)$ are simultaneously equal to zero and construct the $N(\tau)$ plot [Fig. 31(a)]. The location of minimum of $N(\tau)$ allows us to define the delay time accurately, $\tau_1' = 300$. To estimate the parameter ε_1 from time series of the dynamical variable measured between the nonlinear element and the filter (see Fig. 2), we exploit the method proposed in Sec. IV. We filter the time series of $s(t)$ under variation of the filter cut-off frequency $\nu = 1/\varepsilon$ and plot $s(t)$ versus $u(t-\tau_1')$, where $u(t-\tau_1')$ is the signal at the filter output shifted by the time τ_1'. Then, we calculate the length L of a line connecting all points in the plane $[u(t-\tau_1'), s(t)]$ ordered with respect to $u(t-\tau_1')$ and construct the $L(\varepsilon)$ plot [Fig. 31(b)]. For the step of ε variation equal to 0.1, the minimum of $L(\varepsilon)$ is observed at $\varepsilon_1' = 10.0$. For the filter cut-off frequency $\nu_1 = 1/\varepsilon_1$, in the absence of message $u(t-\tau_1) = x(t-\tau_1)$ and the set of points in the plane $(x(t-\tau_1), f(x(t-\tau_1)))$ reproduces the function f. The nonlinear function recovered from $s(t)$ using the estimated τ_1' and ε_1' is shown in Fig. 31(c). We approximated the recovered function with a polynomial of degree 15.

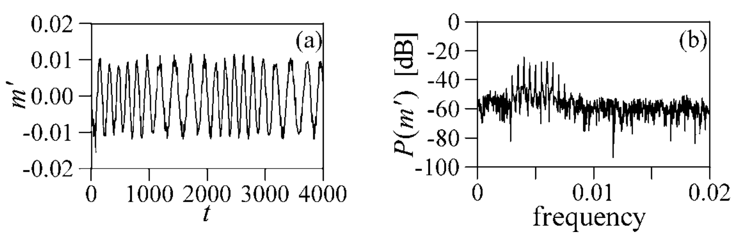

Figure 30. (a) The extracted frequency-modulated harmonic signal for the communication scheme 3/1. (b) The power spectrum of the extracted message signal.

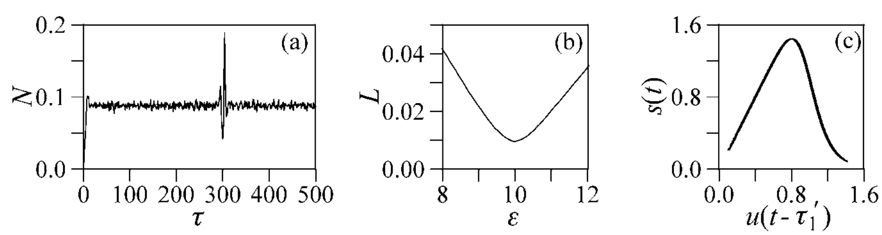

Figure 31. Reconstruction of the transmitter parameters for the case 2/3. (a) The $N(\tau)$ plot. $N(\tau)$ is normalized to the total number of extrema in the time series. $N_{\min}(\tau) = N(300)$. (b) The $L(\varepsilon)$ plot. $L(\varepsilon)$ is normalized to the number of points. $L_{\min}(\varepsilon) = L(10.0)$. (c) The recovered nonlinear function at $\tau_1' = 300$ and $\varepsilon_1' = 10.0$.

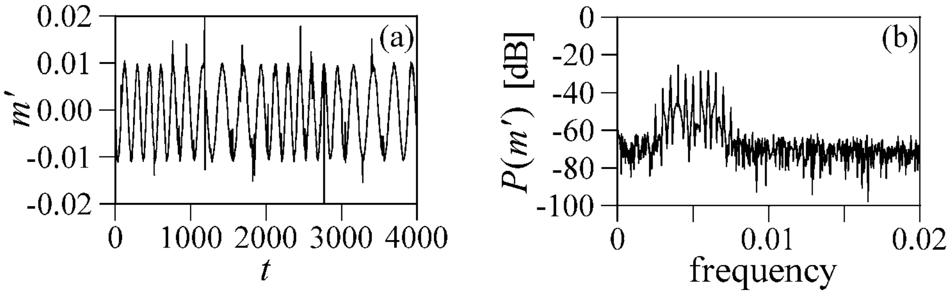

Figure 32. (a) The extracted frequency-modulated harmonic signal for the communication scheme 2/3. (b) The power spectrum of the extracted message signal.

Part of the time series of the extracted information signal calculated using formula (46) and the power spectrum of this extracted signal are presented in Fig. 32. From formula (46) it follows that the message signal may be recovered with a large error at the points where the derivative in the denominator is close to zero. This error can be reduced using frequency filtering of the recovered message signal.

10 Conclusion

We have proposed the methods for reconstructing various classes of time-delay systems from chaotic time series. These methods are based on the statistical analysis of time intervals between extrema in the time series and the projection of infinite-dimensional phase space of the time-delay system to suitably chosen low-dimensional subspaces. The methods can be applied to time-delay systems of different nature if these systems have similar structure of model equations. The proposed techniques allow one to estimate the delay times, the parameters characterizing the inertial properties of the systems, and the nonlinear functions even in the presence of sufficiently high level of noise. The proposed original method of the delay time definition uses only operations of comparing and adding. It needs neither ordering of data, nor calculation of certain measure of complexity of the trajectory or the minimal forecast error of the constructed model and therefore it does not need significant time of computation. For the systems with a single delay time the procedures proposed for the nonlinear function recovery and estimation of the parameters characterizing the inertial properties of the system use all points of the time series in contrast to the methods using only extremal points or points selected according to a certain rule. It allows one to use short time series and to reconstruct the nonlinear function even in the regimes of weakly developed chaos. The methods are successfully applied to recovery of standard time-delay systems from their simulated time series corrupted with noise and to modeling various electronic oscillators with delayed feedback from their experimental time series.

Besides the recovering of the system parameters the proposed methods allow one to determine the a priori unknown order of the time-delay system. We have shown that the model equations of the ring time-delay systems can be reconstructed from time series of various dynamical variables measured at different points of the time-delay system.

We have proposed the method for estimation of coupling between two scalar time-delay systems based on the reconstruction of the model equations of coupled systems from their time series. The method is able to detect the presence of coupling between two time-delay systems, to define the strength and direction of coupling, and to recover the model equations of coupled time-delay systems from chaotic time series under sufficiently high levels of noise. It is shown that the method is applicable to the linear and diffusive types of coupling between time-delay systems. It is also efficient for some types of nonlinear coupling if the coupling term does not contain the unknown functions. The method can be used for the analysis of unidirectional and mutual coupling of time-delay systems and is effective for a wide range of variation of the coupling coefficients even in the case of coupling of principally different time-delay systems. In contrast to the other methods of detection of coupling between the systems from time series the proposed technique is able to define not only the direction but also the value of coupling. It is shown that restricting consideration to several allowed types of coupling it is possible to estimate the coupling coefficients and to recover the coupled systems even in the case where the type of coupling between time-delay systems is a priori unknown. In this case the method allows one to identify the type of coupling. The method efficiency is illustrated using both numerical data, produced by coupled time-delay differential equations including the case of noise presence, and experimental data, gained from coupled electronic oscillators with delayed feedback.

We applied the proposed methods of time-delay system reconstruction to the problem of hidden message extraction in the communication systems with nonlinear mixing of information signal and chaotic signal of a time-delay system. Different ways for encryption and decryption of information in these communication schemes are investigated. We have shown that in the communication systems with nonlinear mixing the hidden message can be successfully extracted from the transmitted signal even in the case when the transmitter parameters are a priori unknown. The procedure of message extraction is based on the method of time-delay systems reconstruction. For different configurations of the transmitter and different measured dynamical variables this method allows one recover the model delay-differential equation of the transmitter from chaotic time series even in the presence of message signal of small amplitude. Thus, even chaotic communication systems with complicated configuration, where the information signal is injected into the feedback circuit of the transmitter with delay-induced dynamics at one point and transmitted into the communication channel from another point, can be successfully unmasked. Hence, the communication systems using chaotic signals of time-delay systems are not as secure as expected in spite of very high dimension and large number of positive Lyapunov exponents of chaotic attractors of time-delay systems.

For different configurations of the transmitter we have demonstrated the extraction of hidden message from the transmitted signal using both numerical data, produced by nonlinear mixing of chaotic signal of the Mackey-Glass system and frequency-modulated harmonic signal, and experimental data, produced by nonlinear mixing of harmonic signal and chaotic signal of the electronic oscillator with delayed feedback. A possible way to improve the level of security of the considered chaotic communication systems is to use modulation of their parameters or to employ high-dimensional time-delay systems.

Acknowledgements

This work is supported by the Russian Foundation for Basic Research, Grants No. 05–02–16305 and No. 07–02–00589. ASK acknowledges support from the “Dynasty” Foundation.

References

[1] Hale, J. K.; Lunel, S. M. V. *Introduction to Functional Differential Equations*; Springer: New York, 1993.
[2] Kuang, Y. *Delay Differential Equations With Applications in Population Dynamics*; Academic Press: Boston, 1993.
[3] Ikeda, K.; Matsumoto, K. *Physica D* 1987 *vol.29*, 223-235.
[4] Ikeda, K. *Opt. Commun.* 1979 *vol.30*, 257-261.
[5] Lang, R.; Kobayashi, K. *IEEE J. Quantum Electron.* 1980 *vol.16*, 347-355.
[6] Mackey, M. C.; Glass, L. *Science* 1977 *vol.197*, 287-289.
[7] Bocharov, G. A.; Rihan, F. A. *J. Comp. Appl. Math.* 2000 *vol.125*, 183-199.
[8] Farmer, J. D. *Physica D* 1982 *vol.4*, 366-393.
[9] Fowler, A. C.; Kember, G. *Phys. Lett. A* 1993 *vol.175*, 402-408.
[10] Hegger, R.; Bünner, M. J.; Kantz, H.; Giaquinta, A. *Phys. Rev. Lett.* 1998 *vol.81*, 558-561.
[11] Zhou, C.; Lai, C.-H. *Phys. Rev. E* 1999 *vol.60*, 320-323.
[12] Udaltsov, V. S.; Goedgebuer, J.-P.; Larger, L.; Cuenot, J.-B.; Levy, P.; Rhodes, W. T. *Phys. Lett. A* 2003 *vol.308*, 54-60.
[13] Tian, Y.-C.; Gao, F. *Physica D* 1997 *vol.108*, 113-118.
[14] Kaplan, D. T.; Glass, L. *Physica D* 1993 *vol.64*, 431-454.
[15] Bünner, M. J.; Popp, M.; Meyer, Th.; Kittel, A.; Rau, U.; Parisi, J. *Phys. Lett. A* 1996 *vol.211*, 345-349.
[16] Bünner, M. J.; Popp, M.; Meyer, Th.; Kittel, A.; Parisi, J. *Phys. Rev. E* 1996 *vol.54*, 3082-3085.
[17] Bünner, M. J.; Meyer, Th.; Kittel, A.; Parisi, J. *Phys. Rev. E* 1997 *vol.56*, 5083-5089.
[18] Bünner, M. J.; Ciofini, M.; Giaquinta, A.; Hegger, R.; Kantz, H.; Meucci, R.; Politi, A. *Eur. Phys. J. D* 2000 *vol.10*, 165-176.
[19] Voss, H.; Kurths, J. *Phys. Lett. A* 1997 *vol.234*, 336-344.
[20] Ellner, S. P.; Kendall, B. E.; Wood, S. N.; McCauley, E.; Briggs, C. J. *Physica D* 1997 *vol.110*, 182-194.
[21] Voss, H.; Kurths, J. *Chaos Solitons Fractals* 1999 *vol.10*, 805-809.
[22] Bezruchko, B. P.; Karavaev, A. S.; Ponomarenko, V. I.; Prokhorov, M. D. *Phys. Rev. E* 2001 *vol.64*, 056216.
[23] Ponomarenko, V. I.; Prokhorov, M. D. *Phys. Rev. E* 2002 *vol.66*, 026215.
[24] Prokhorov, M. D.; Ponomarenko, V. I.; Karavaev, A. S.; Bezruchko, B. P. *Physica D* 2005 *vol.203*, 209-223.
[25] Prokhorov, M. D.; Ponomarenko, V. I. *Phys. Rev. E* 2005 *vol.72*, 016210.
[26] Pyragas, K. *Int. J. Bif. Chaos* 1998 *vol.8*, 1839-1842.
[27] Mensour, B.; Longtin, A. *Phys. Lett. A* 1998 *vol.244*, 59-70.

[28]Li, C.; Liao, X.; Wong, K. *Physica D* 2004 *vol.194*, 187-202.
[29]Kye, W.-H.; Choi, M.; Kim, C.-M.; Park, Y.-J. *Phys. Rev. E* 2005 *vol.71*, 045202.
[30]Bai, E.-W.; Lonngren, K. E.; Uçar, A. *Chaos Solitons Fractals* 2005 *vol.23*, 1071-1076.
[31]Udaltsov, V. S.; Goedgebuer, J.-P.; Larger, L.; Rhodes, W. T. *Phys. Rev. Lett.* 2001 *vol.86*, 1892-1895.
[32]Koryukin, I. V.; Mandel, P. *Phys. Rev. E* 2002 *vol.65*, 026201.
[33]Shahverdiev, E. M.; Sivaprakasam, S.; Shore, K. A. *Phys. Rev. E* 2002 *vol.66*, 017206.
[34]Song, Y.; Han, M.; Peng, Y. *Chaos Solitons Fractals* 2004 *vol.22*, 1139-1148.
[35]Seidel, H.; Herzel, H. *Physica D* 1998 *vol.115*, 145-160.
[36]Kotani, K.; Takamasu, K.; Ashkenazy, Y.; Stanley, H. E.; Yamamoto, Y. *Phys. Rev. E* 2002 *vol.65*, 051923.
[37]Rosenblum, M. G.; Pikovsky, A. S. *Phys. Rev. E* 2001 *vol.64*, 045202.
[38]Rosenblum, M. G.; Cimponeriu, L.; Bezerianos, A.; Patzak, A.; Mrowka, R. *Phys. Rev. E* 2002 *vol.65*, 041909.
[39]Smirnov, D. A.; Bezruchko, B. P. *Phys. Rev. E* 2003 *vol.68*, 046209.
[40]Pecora, L. M.; Carroll, T. L. *Phys. Rev. Lett.* 1990 *vol.64*, 821-824.
[41]Kocarev, L.; Halle, K. S.; Eckert, K.; Chua, L. O.; Parlitz, U. *Int. J. Bif. Chaos* 1992 *vol.2*, 709-713.
[42]Cuomo, K. M.; Oppenheim, A. V. *Phys. Rev. Lett.* 1993 *vol.71*, 65-68.
[43]Dmitriev, A. S.; Panas, A. I.; Starkov, S. O. *Int. J. Bif. Chaos* 1995 *vol.5*, 1249-1254.
[44]Pecora, L. M.; Carroll, T. L.; Johnson, G. A.; Mar, D. J.; Heagy, J. F. *Chaos* 1997 *vol.7*, 520-543.
[45]Pérez, G.; Cerdeira, H. A. *Phys. Rev. Lett.* 1995 *vol.74*, 1970-1973.
[46]Short, K. M. *Int. J. Bif. Chaos* 1997 *vol.7*, 1579-1597.
[47]Zhou, C.-S.; Chen, T.-L. *Phys. Lett. A* 1997 *vol.234*, 429-435.
[48]Yang, T.; Yang, L.-B.; Yang, C.-M. *Phys. Lett. A* 1998 *vol.247*, 105-111.
[49]Álvarez, G.; Montoya, F.; Pastor, G.; Romera, M. *Chaos* 2004 *vol.14*, 274-278.
[50]Voss, H. U. *Phys. Rev. E* 2000 *vol.61*, 5115-5119.